Simulating tracking devices relying on ionisation, gas-based detectors in particular

ionisation process

field calculations

electron transport

signal induction

Trends in tracking

- Intrinsic resolution:
  - MWPC: ~1 mm detect wire hit
  - drift chambers: 150-250 μm measure drift time
  - LHC experiments: 50-200 μm gas, electronics ...
  - micropattern detectors: 20- 50 μm small scale electrodes
  - semi-conductors: a few μm
- Relying on increasingly subtle sensitive medium properties.
- Better and better understanding of the operating principles.

Helios/I tracking (1989)

- Three kinds of devices:
  - silicon strips near the vertex;
  - innovative drift chambers with CO_2 80 % Ar 20 %, 150-200 μm resolution;
  - large area multi-wire proportional chambers far downstream.

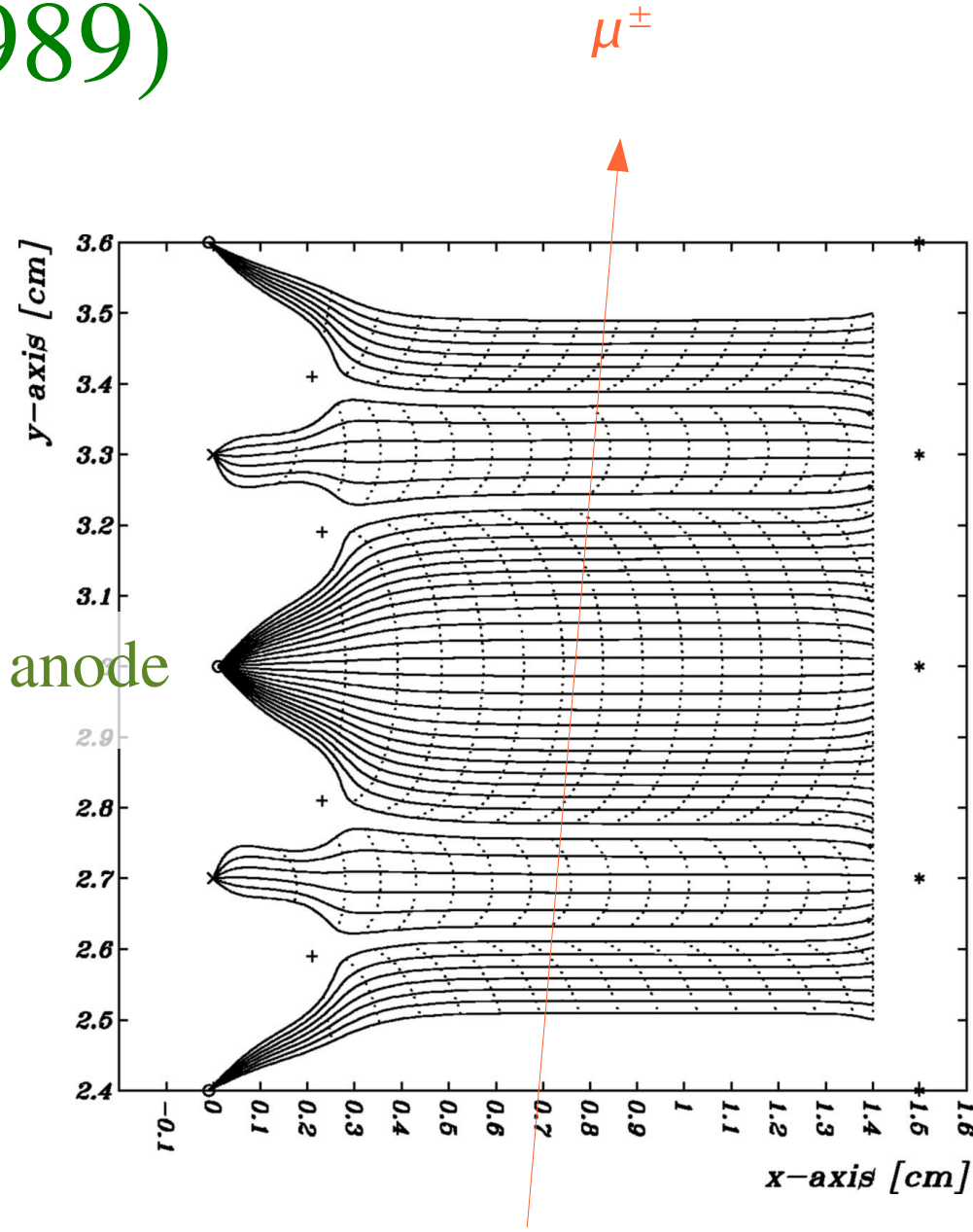

Atlas $\mu^{\pm}$ chambers (MDT)

Atlas MDT resolution

- Tube resolution is sensitive to:
  - details of ionisation patterns,
  - spatial extent δ-electrons,
  - e^- transport and diffusion,
  - gain and space charge,
  - resistor noise, t_p, filters ...
- Detector optimised combining test runs & detailed simulation.

- Reference: Werner Riegler, PhD thesis. Graphs for Ar 91 %, N_2 4 %, CH_4 5 % at 3 bar, which is not the mixture that will be used.

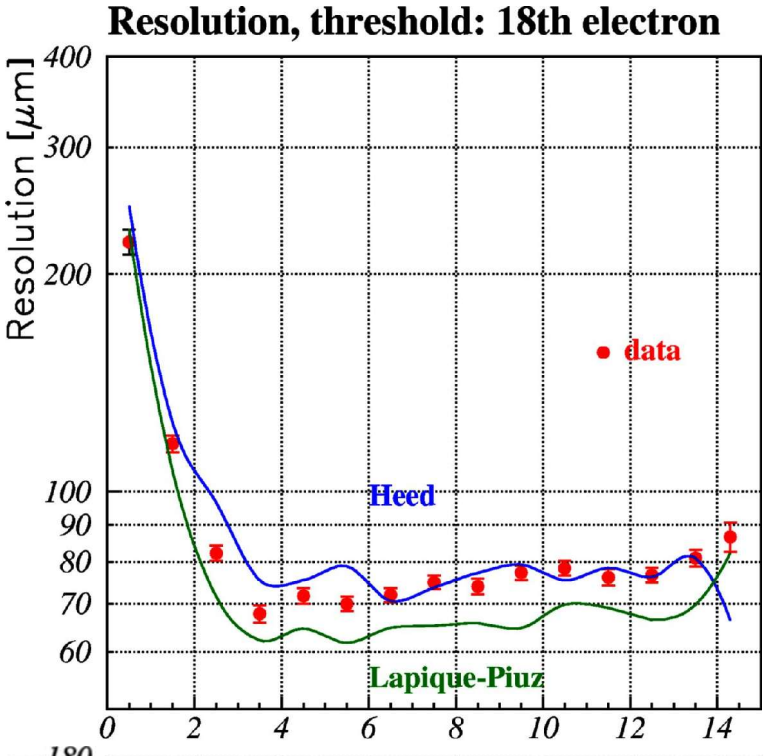

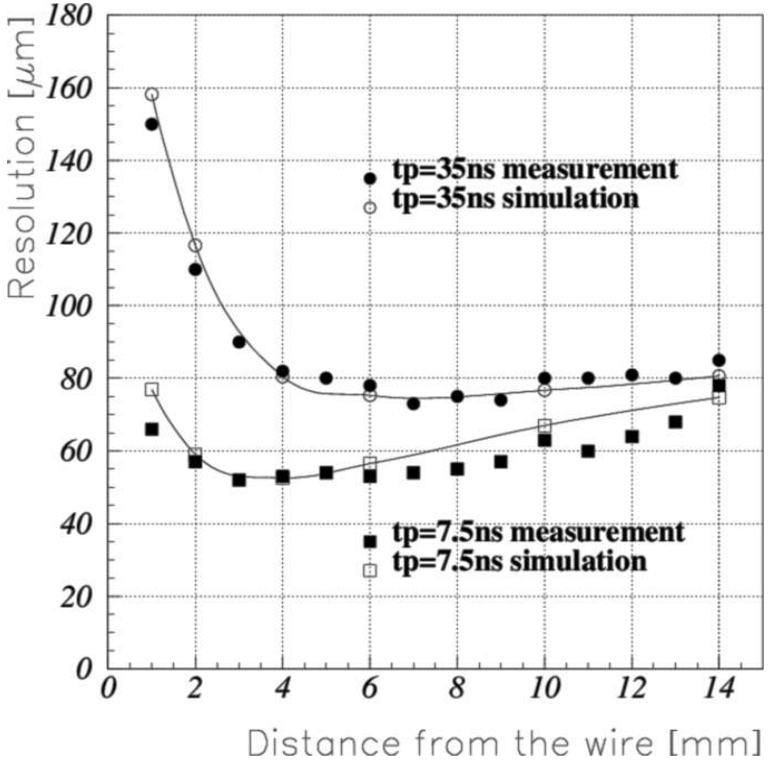

Future: Micromegas

- Fast, rate tolerant tracking device
- 1994: Yannis Giomataris and Georges Charpak

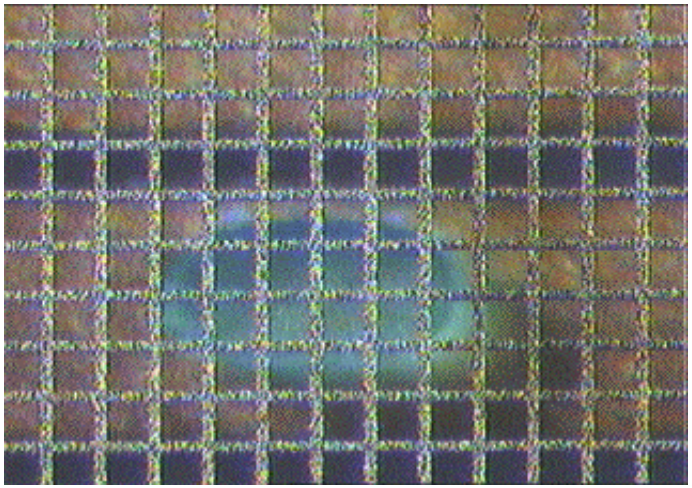

A mesh – holes of 30 μm

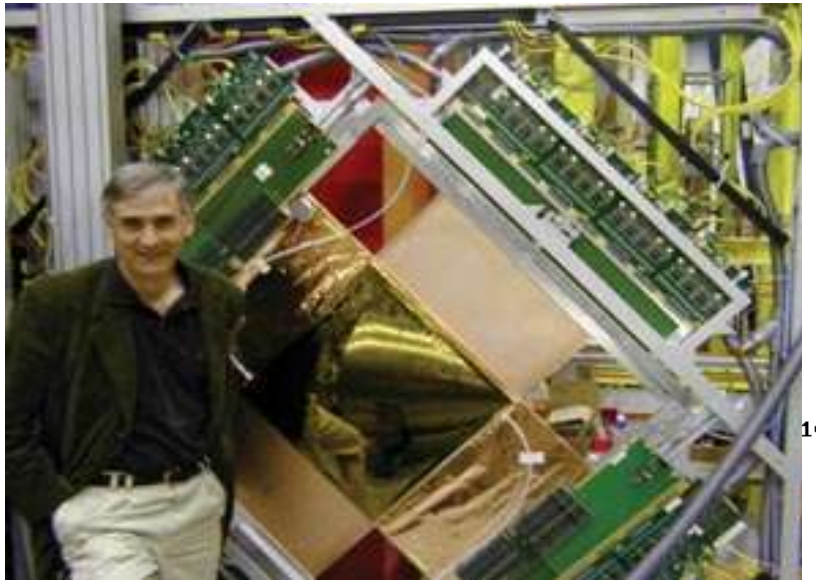

Yannis Giomataris

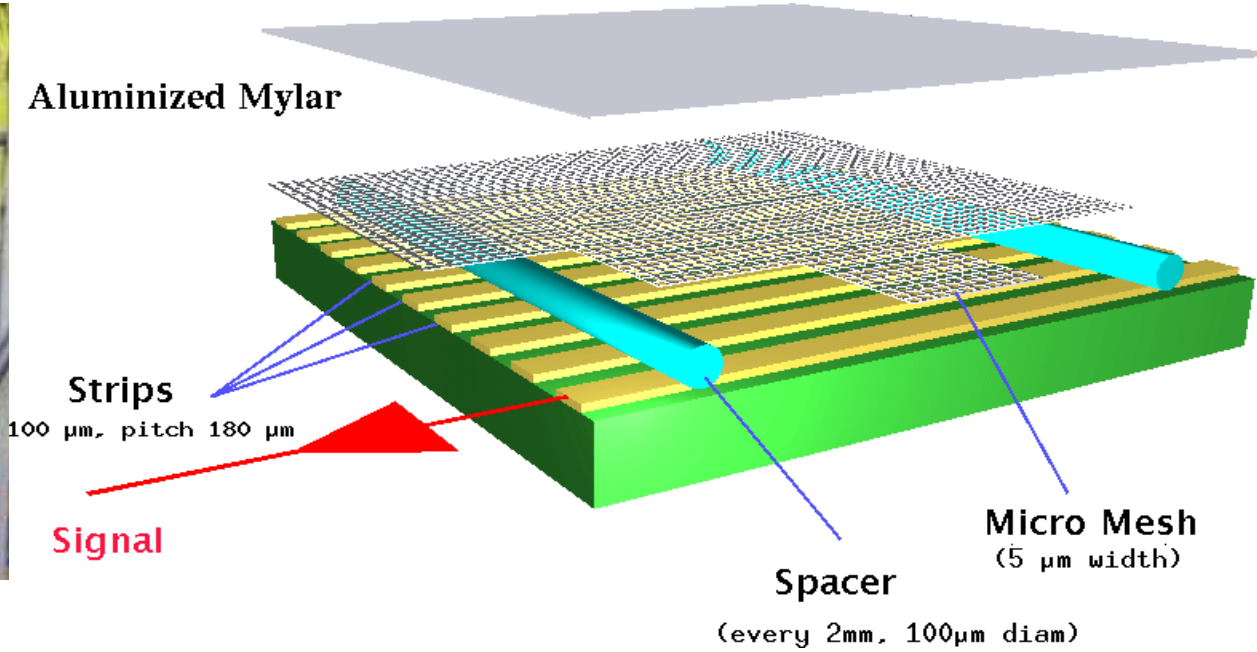

Future: GEMs

- Acts as a “pre-amplifier”
- 1996: Fabio Sauli

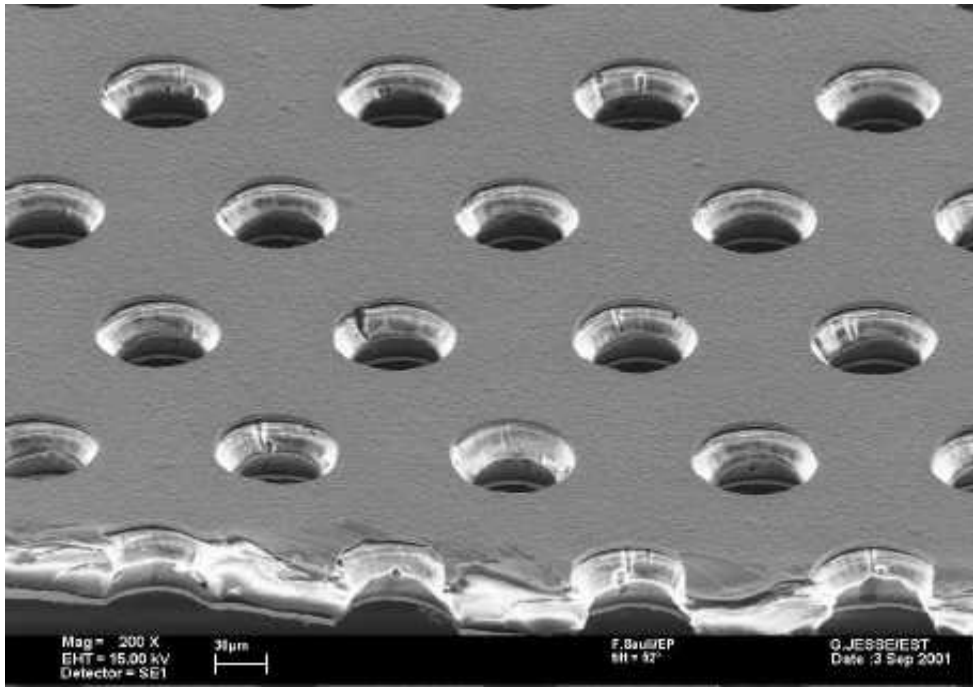

A few electrons enter here

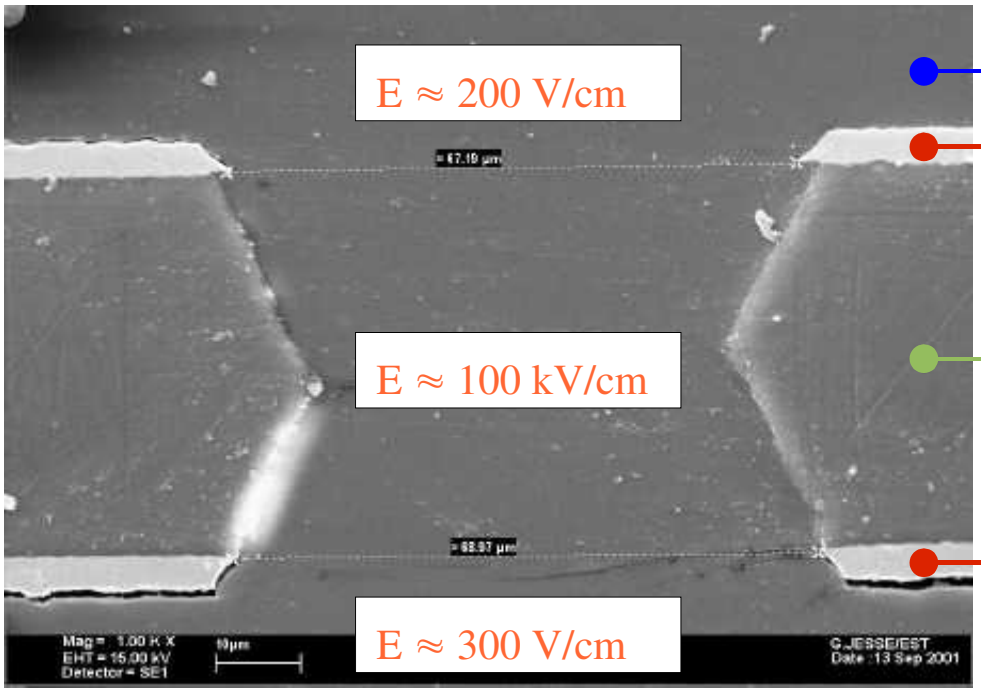

Gas

Metal

Dielectric

Metal

Fabio Sauli

Many electrons exit here

Principles of ionisation-based tracking

- These devices work according to similar principles:
  - a charged particle passing through the gas ionises some of the gas molecules;
  - the electric field in the gas volume transports the ionisation electrons and, in some areas, also provokes multiplication;
  - the charge movements (of electrons and ions) lead to induced currents in electrodes, and these currents are recorded.

Ionisation processes: Heed

Igor Smirnov

- PAI model or absorption of real photons:

  $Atom + \pi^- \rightarrow Ion^{+*} + \pi^- + e^-$

  $Atom + \gamma \rightarrow Ion^{+*} + e^-$ (photo-electric effect)

- Decay of excited states:

  $Ion^{+*} \rightarrow Ion^{++} + e^-$ (Auger)

  $Ion^{+*} \rightarrow Ion^{+} + \gamma$ (fluorescence)

  $Ion^{+*} \rightarrow Ion^{+*}$ (Coster-Kronig)

- Treatment of:
  - secondary photons, returning to the PAI model,
  - ionising photo-electrons and Auger-electrons, collectively known as δ-electrons:

  $e^- + Atom \rightarrow Ion^{+} + 2\, e^-$ (absorption of high-energy electrons)

Basic formulae of the PAI model

- Key ingredient: photo-absorption cross section $\sigma_\gamma(E)$

$$\frac{\beta^2\pi}{\alpha}\frac{\mathrm{d}\sigma}{\mathrm{d}E}=\frac{\sigma_\gamma(E)}{E}\log\left(\frac{1}{\sqrt{(1-\beta^2\epsilon_1)^2+\beta^4\epsilon_2^2}}\right)+$$ Relativistic rise

Cross section to transfer energy E

$$\frac{1}{N\bar{h}c}\left(\beta^2-\frac{\epsilon_1}{|\epsilon|^2}\right)\theta+$$ Čerenkov radiation

$$\frac{\sigma_\gamma(E)}{E}\log\left(\frac{2m_e c^2\beta^2}{E}\right)+$$ Resonance region

$$\frac{1}{E^2}\int_0^E\sigma_\gamma(E_1)\,\mathrm{d}E_1$$ Rutherford scattering

With: $\epsilon_2(E)=\frac{N_e\bar{h}c}{EZ}\sigma_\gamma(E)$

$$\epsilon_1(E)=1+\frac{2}{\pi}\mathrm{P}\int_0^\infty\frac{x\,\epsilon_2(x)}{x^2-E^2}\mathrm{d}x$$

$$\theta=\arg(1-\epsilon_1\beta^2+i\,\epsilon_2\beta^2)=\frac{\pi}{2}-\arctan\frac{1-\epsilon_1\beta^2}{\epsilon_2\beta^2}$$

Energy Loss (PAI Model)

optical loss function Im(-1/$\epsilon(E)$) of solid Si

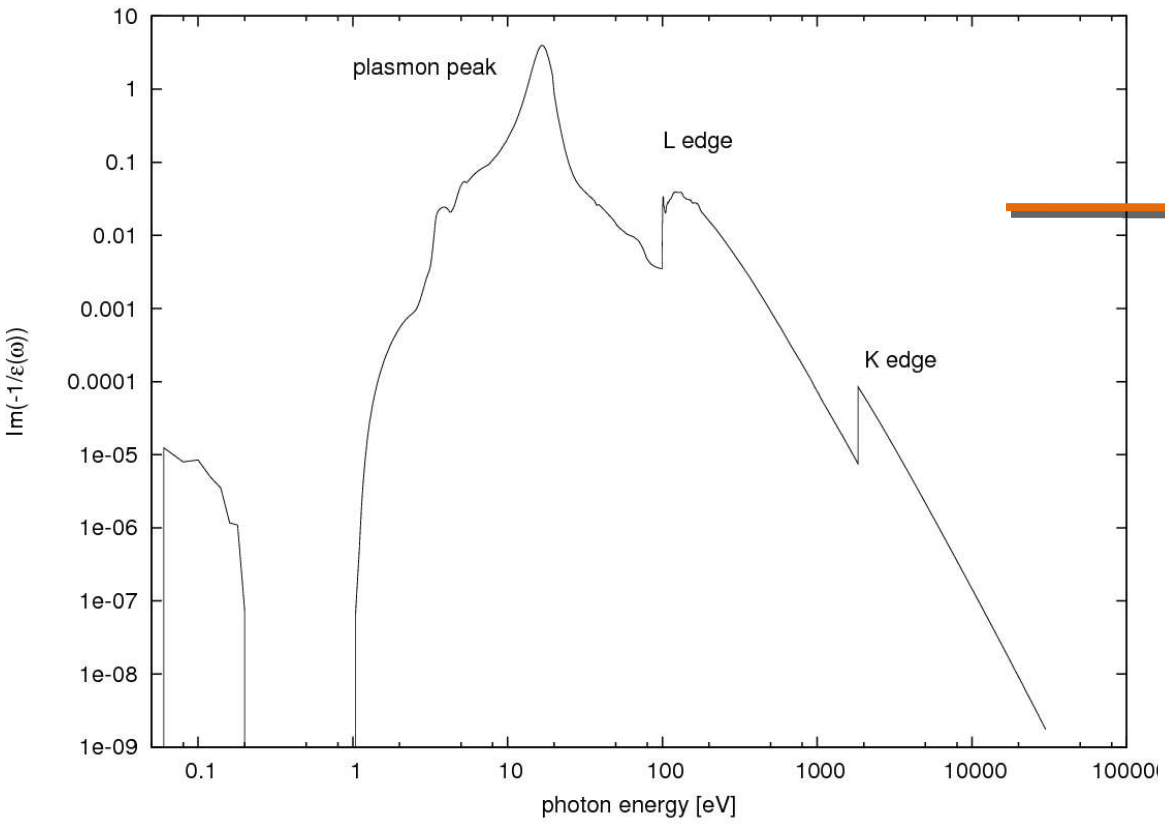

differential cross-section

$$\frac{\mathrm{d}\sigma}{\mathrm{d}E} = \left(\frac{z^2\alpha_f}{\beta^2\pi N_{\mathrm{el}}\hbar c}\right)\mathrm{Im}\frac{-1}{\epsilon(E)}\log\frac{2m\beta^2c^2}{E|1-\beta^2\epsilon(E)|} +$$

$$\left(\frac{z^2\alpha_f}{\beta^2\pi N_{\mathrm{el}}\hbar c}\right)\left(\beta^2 - \frac{\epsilon'(E)}{|\epsilon(E)|^2}\right)\left(\frac{\pi}{2} - \arctan\frac{1-\beta^2\epsilon'(E)}{\beta^2\epsilon''(E)}\right) +$$

$$\left(\frac{z^2\alpha_f}{\beta^2\pi N_{\mathrm{el}}\hbar c}\right)\frac{1}{E^2}\int_0^{\epsilon} E'\,\mathrm{Im}\frac{-1}{\epsilon(E')}\,\mathrm{d}E'$$

$$\left(\sigma(E) \rightarrow \mathrm{Im}\frac{-1}{\epsilon(E)}\right)$$

loss spectrum (5 GeV/c π, 20.5 μm Si)

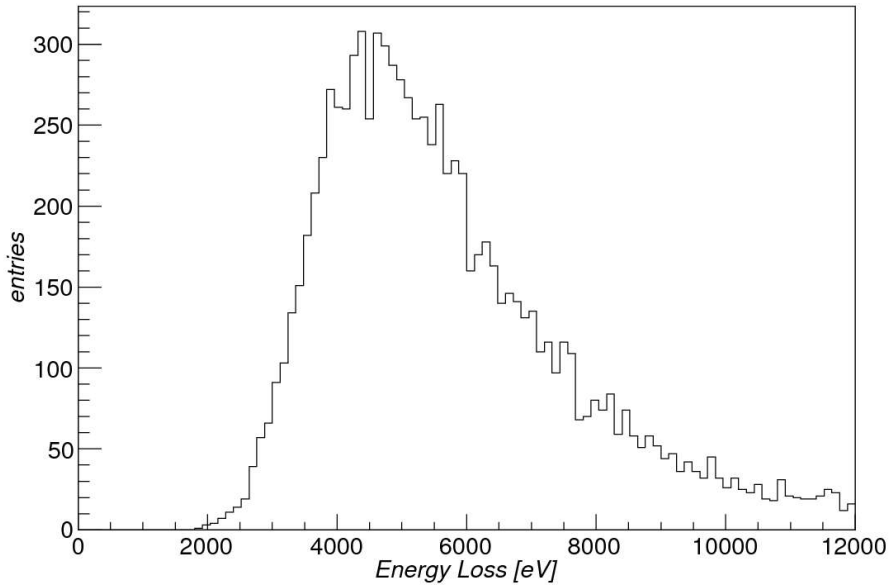

Primary Ionization: calculate number of e/h pairs from $W = 3.6$ eV, $F \approx 0.12$ or perform detailed simulation of secondary electron cascade

How well is the cross section known ?

- Much worse agreement at the shell borders !

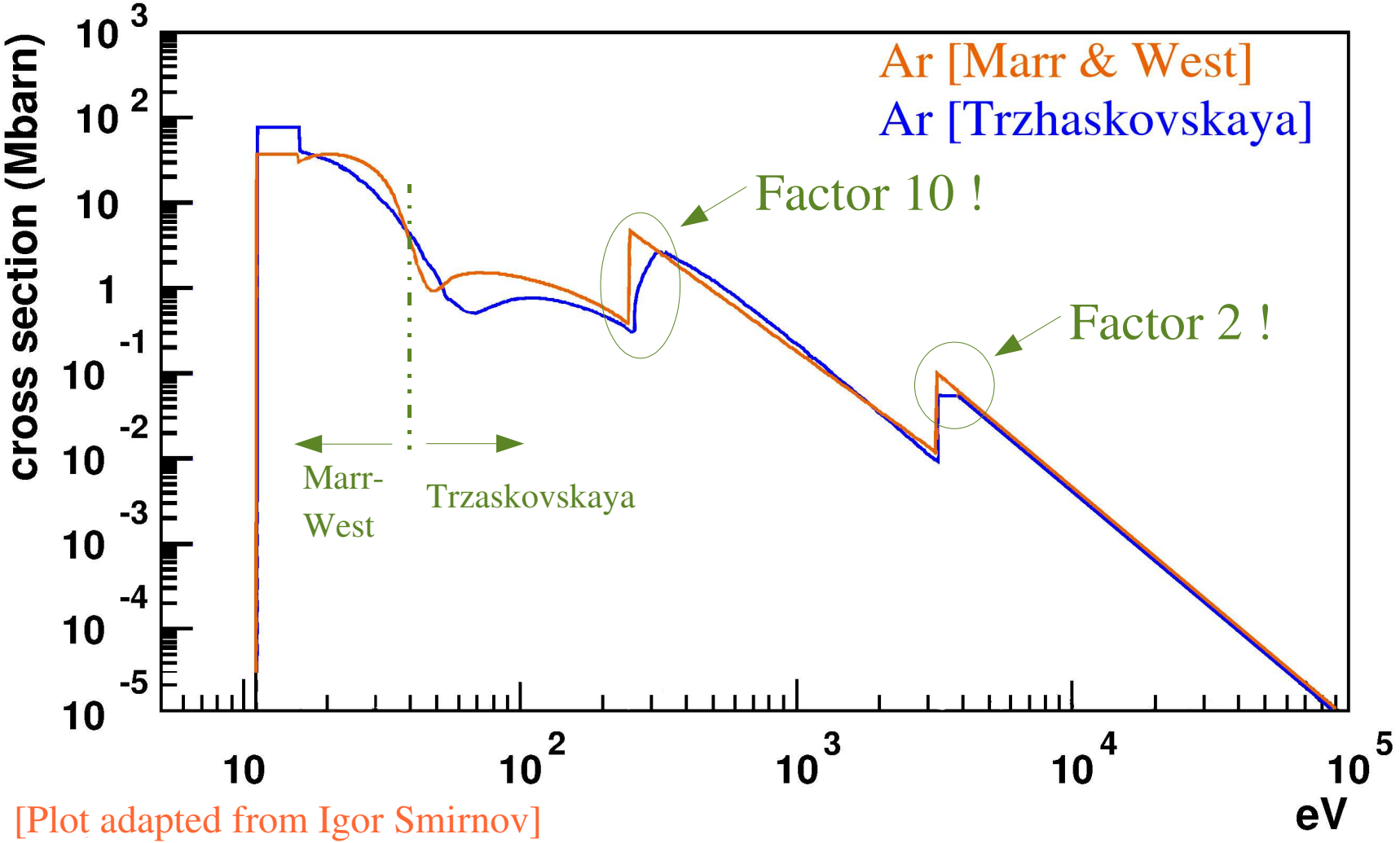

[Plot adapted from Igor Smirnov]

Efficiency of the CAST TPC

- Field cage depth: ~10 cm.
- Filled with Ar 95% + CH_4 5%.

- Efficiency measurements at the Panter facility (München) for 0.27 keV < E_γ < 8.05 keV.

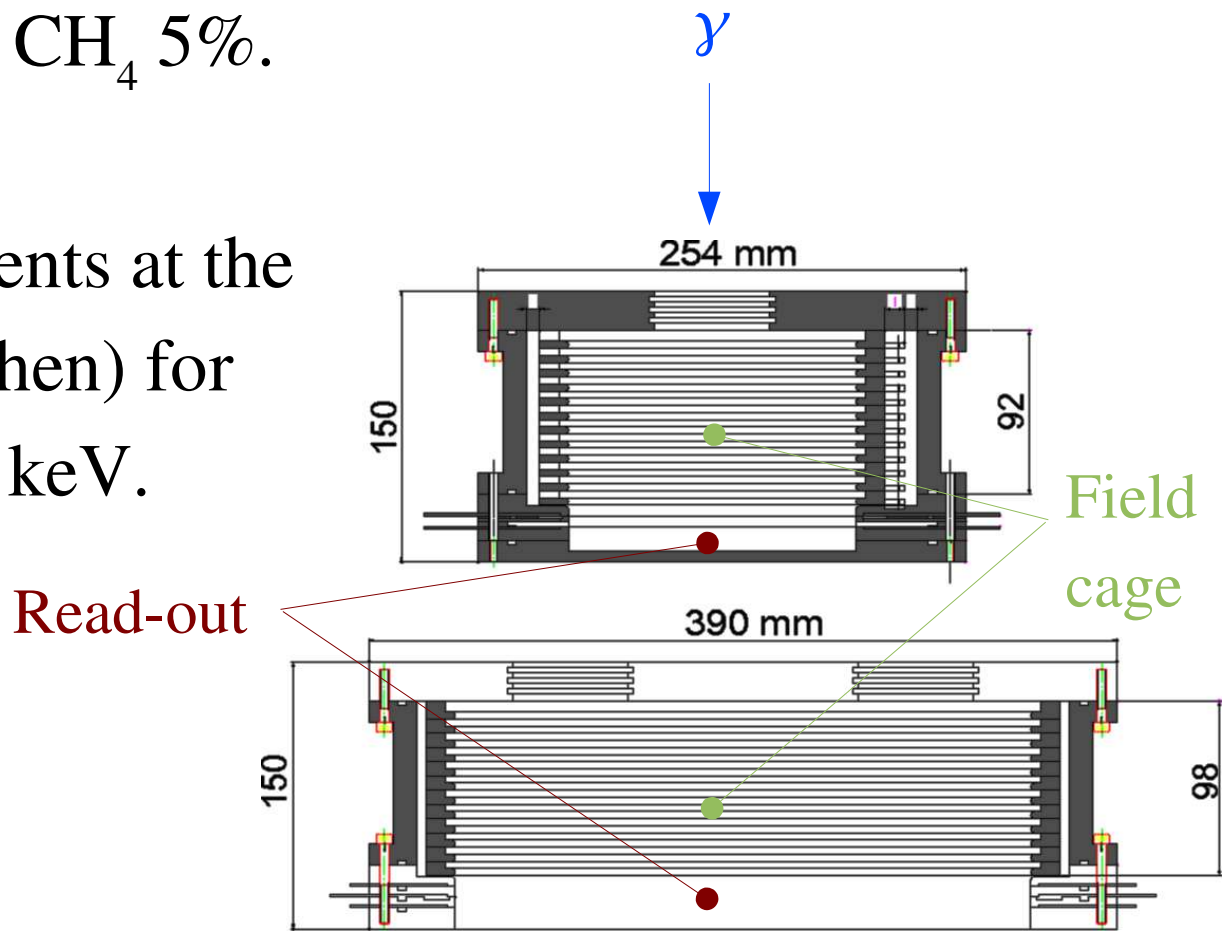

[Plot adapted from CAST]

Understanding the efficiency

- CAST sees a 30 % drop in efficiency at 3 keV, i.e. the argon K-shell (3.2 keV).
  - Henke: $\lambda = 3$ cm: 5 %,
  - Heed: $\lambda = 7$ cm: 28 %.
- $E_\gamma > 3.2$ keV: 2.95 keV fluorescence γ emission can occur which can cause secondary ionisation.

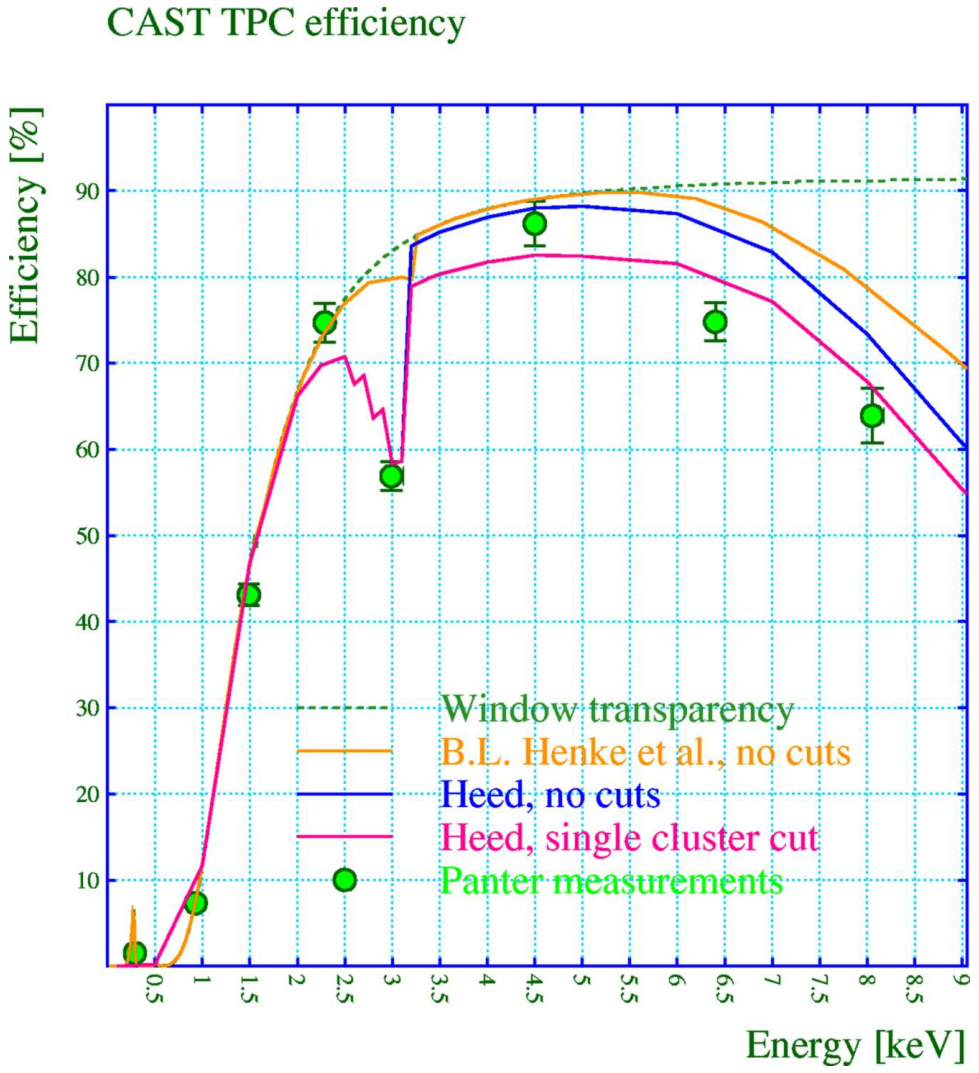

RPC

- Widely used triggering device
- Excellent timing resolution
- Can cover huge areas
- Also as multiple-gap version

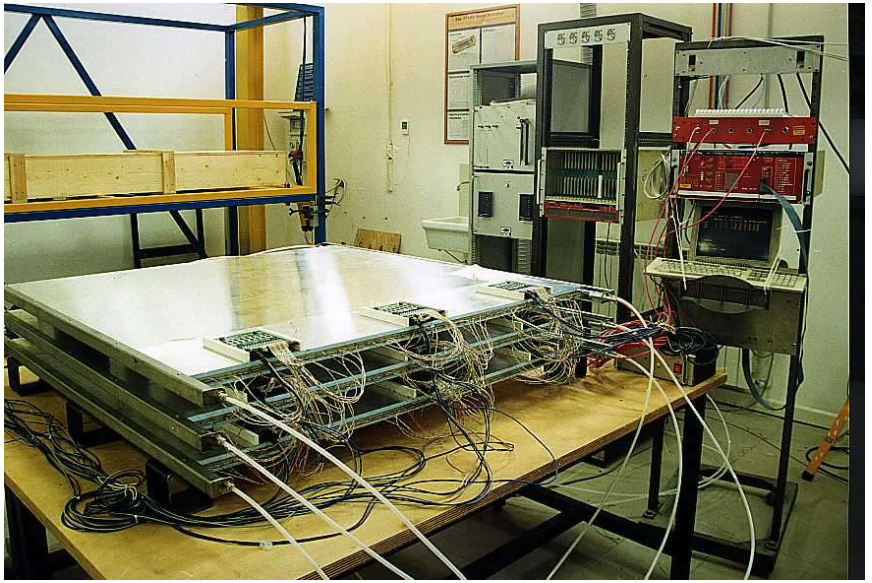

An Atlas RPC module

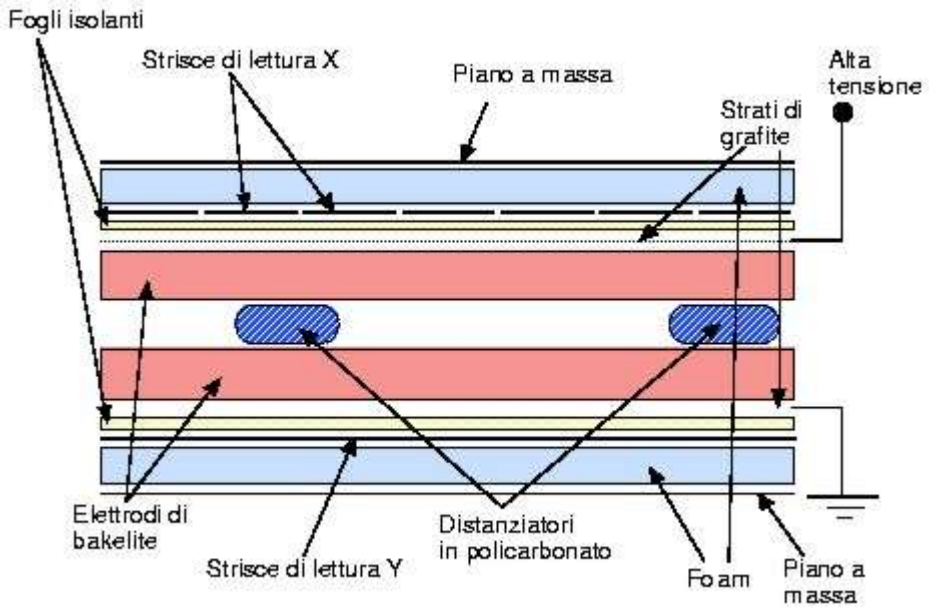

The RPC efficiency puzzle

- An RPC with a gap of 300 μm has a typical efficiency of 75 %.
- This is hopelessly incompatible with popular, large, spacings of primary interactions - exotic scenarios have been put forward ...
- It fits perfectly however with the smaller spacings seen in some measurements and also with Heed.
- [Werner Riegler *et al., Detector physics and simulation of resistive plate chambers*, NIM A **500** (2003) 144-162.]

Spacing of primary interactions

- Disagreement of a factor of ≈2 in the number of primary interactions per cm.

- Sources:
  - F. F. Rieke & W. Prepejchal, Phys. Rev. A **6** (1972) 1507-1519.
  - F. Sauli, CERN 77-09(1977).
  - J. Fischer *et al.*, NIM A **238** (1985) 249-264.

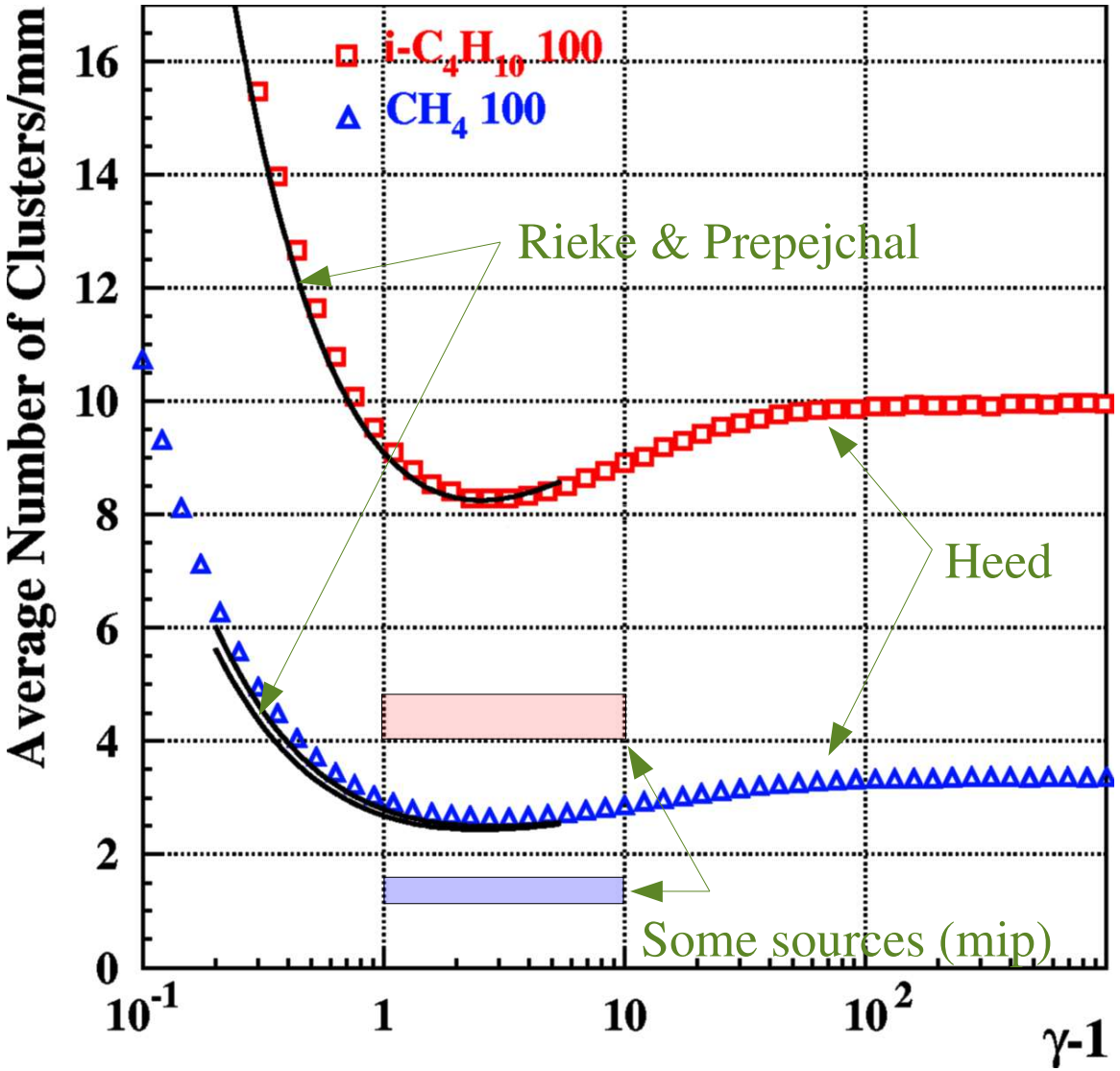

[Adapted from: W. Riegler *et al.*, NIM A **500** (2003) 144-162.]

Photo-absorption in xenon

- Same features as argon, but for 5 shells:

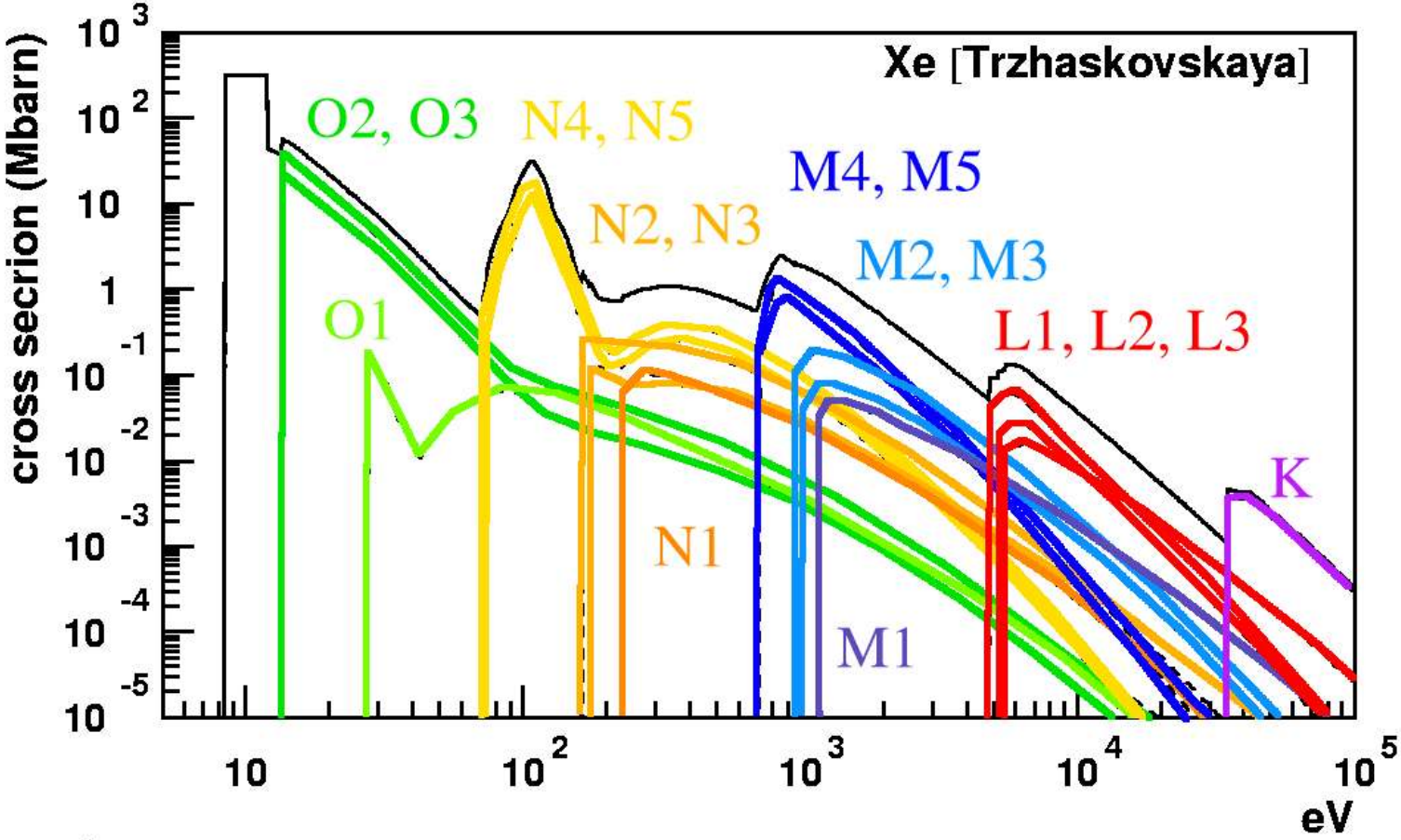

[Plot from Igor Smirnov]

De-excitation

Ralph de Laer Kronig
(1904-1995)

Liese Meitner
(1878-1968)

Pierre Victor Auger
(1899-1993)

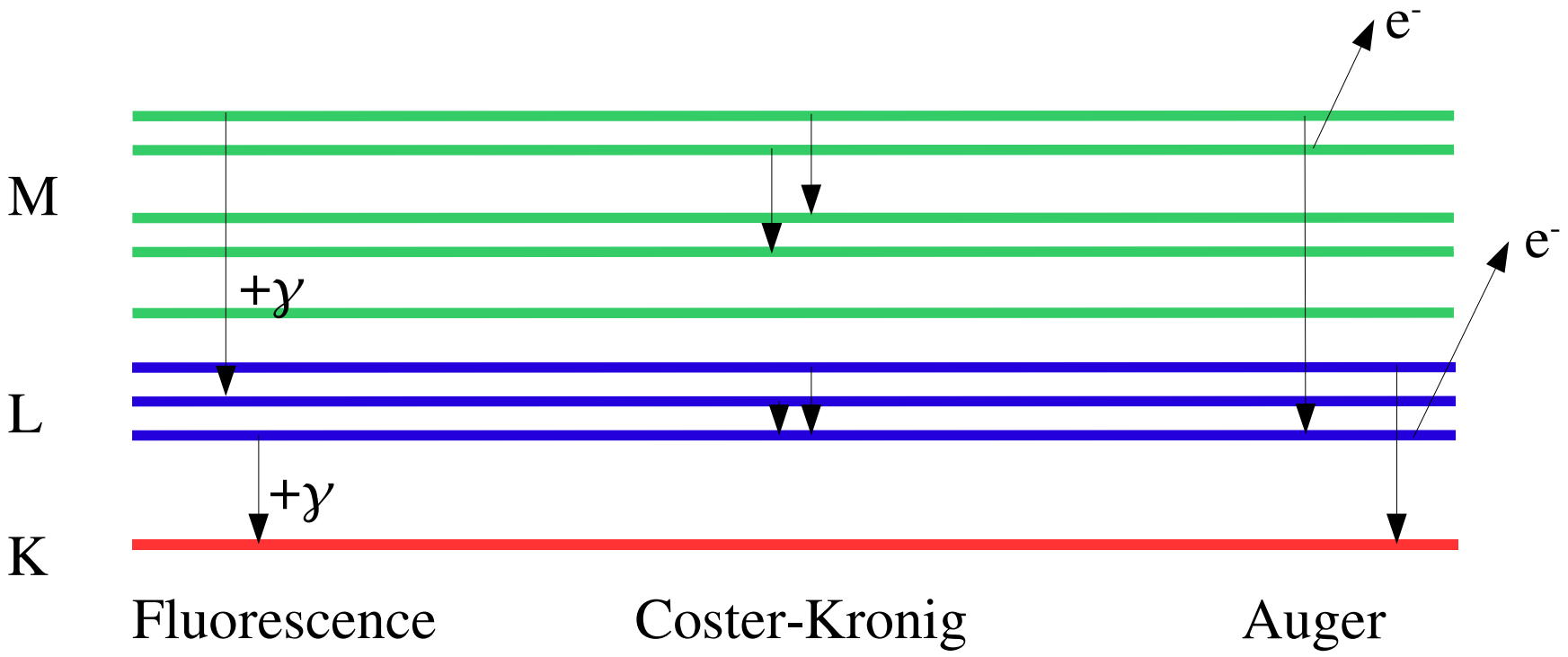

References:

D. Coster and R. de L. Kronig, Physica **2** (1935) 1, 13.

L. Meitner, *Das beta-Strahlenspektrum von UX1 und seine Deutung*, Z. Phys. **17** (1923) 54-66.

P. Auger, J. Phys. Radium **6** (1925) 205.

Filling the L shell

- L_1 (rare): Coster-Kronig followed by Auger e^-.
- L_2 and L_3 (dominant): Auger e^- or fluorescence.
- Uncertainties: ± 15-20 % for Coster-Kronig and ± 20-30 % for fluorescence and Auger e^-.

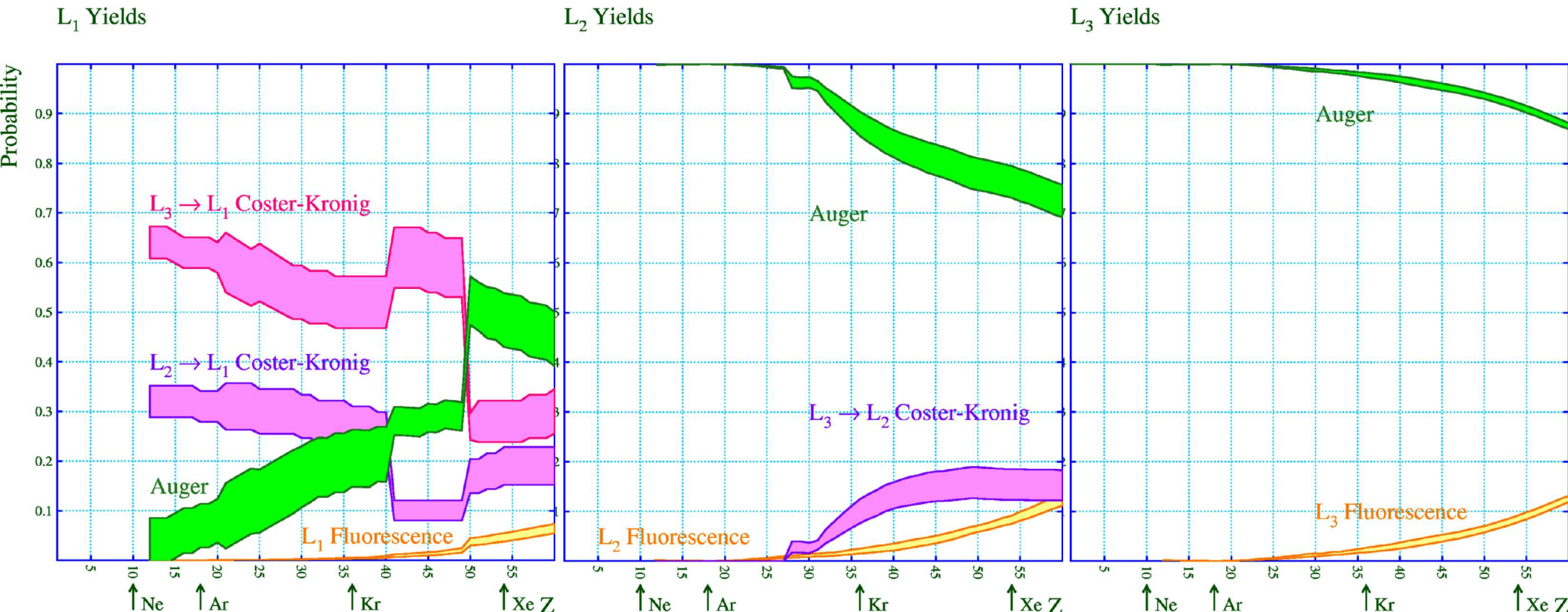

Photo- & Auger-electrons

- Assuming we can simulate the production of photo- and Auger electrons (together called δ-electrons):
  - How far does a δ-electron travel ?
    - Affects the spatial resolution.
  - What is the distribution of the number of low energy (secondary) electrons produced by a single δ-electron ?
    - A factor in the signal amplitude.

Range of photo- and Auger-electrons

- Electrons scatter in a gas.
- Measures of the range:
  - R_{total}: total path length
  - R_p: practical range
  - $\bar{z}$: cog in direction of initial motion
  - σ_z: RMS in direction of initial motion
  - σ_x: RMS transverse to initial motion

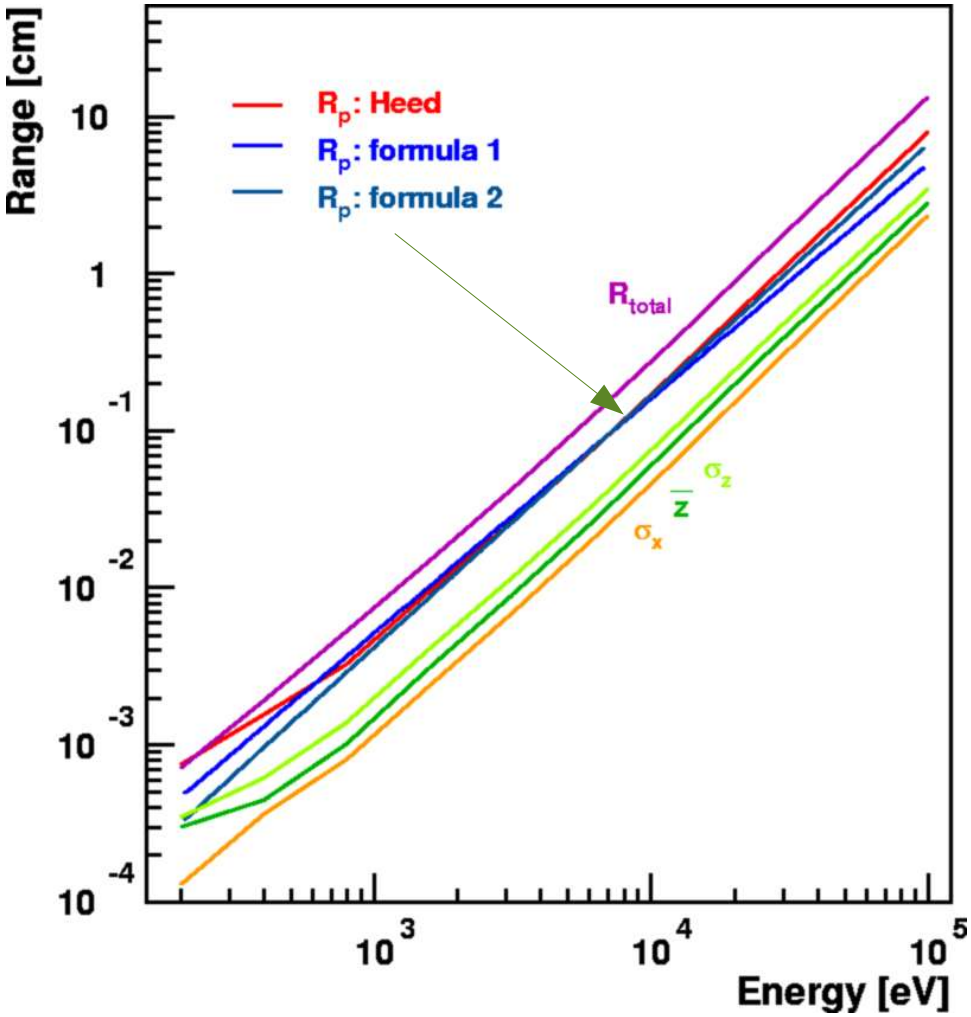

Practical range: distance at which the tangent through the inflection point of the descending portion of the depth- absorbed dose curve meets the extrapolation of the Bremsstrahlung background (ICRU report 35, 1984)

Number of electrons produced

- The distribution of the number of electrons n_e created by a photo- or Auger-electron with energy E_δ is characterised by:
  - the mean of n_e, given by the average work w needed to produce one electron:
    $\bar{n}_e = E_\delta / w(E_\delta)$
  - the spread of n_e, given by the so-called Fano factor F:
    $\sigma^2(n_e) = F(E_\delta)\,\bar{n}_e$

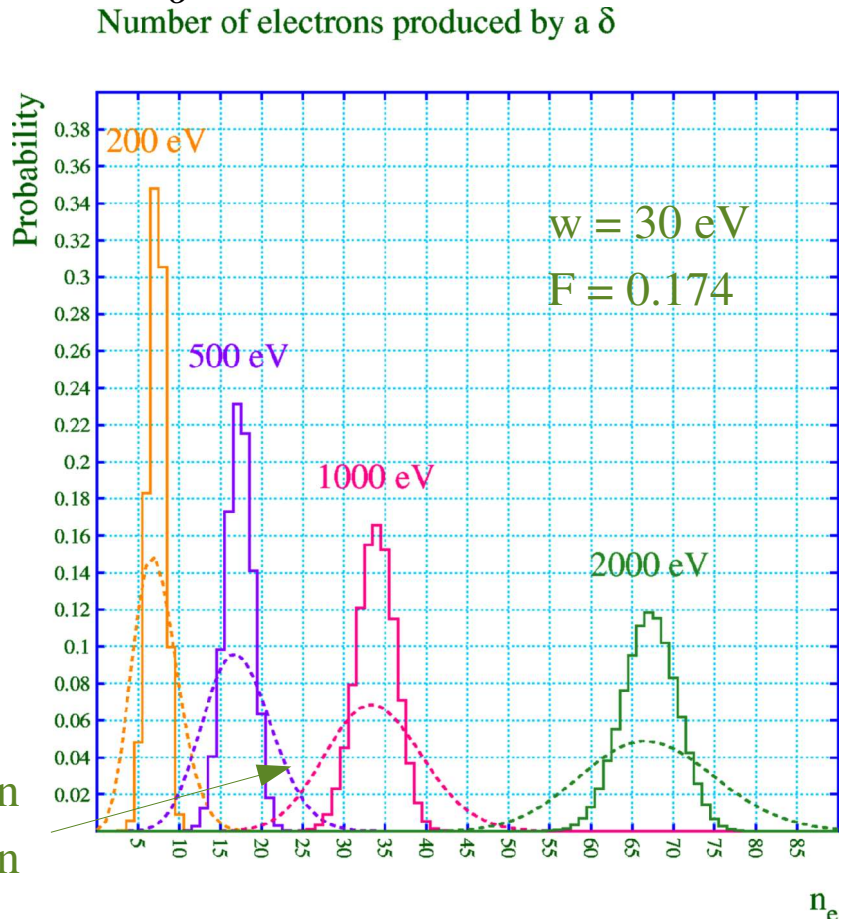

Data on electron deposition

- Data and calculations exist, but the spread (≈10 %) is larger than the measurement errors (1-4 %).

Gas	w [eV]	F
He	41.3-43.3	0.21
Ne	35.4	0.13
Ar	26.3-26.4	0.16
Kr	24.4	0.17-0.19
Xe	21.9-22.1	0.13-0.17
CO_2	33.0-37.2	0.33
CH_4	34.3	0.265-0.285
C_2H_6	11.5	0.250-0.280

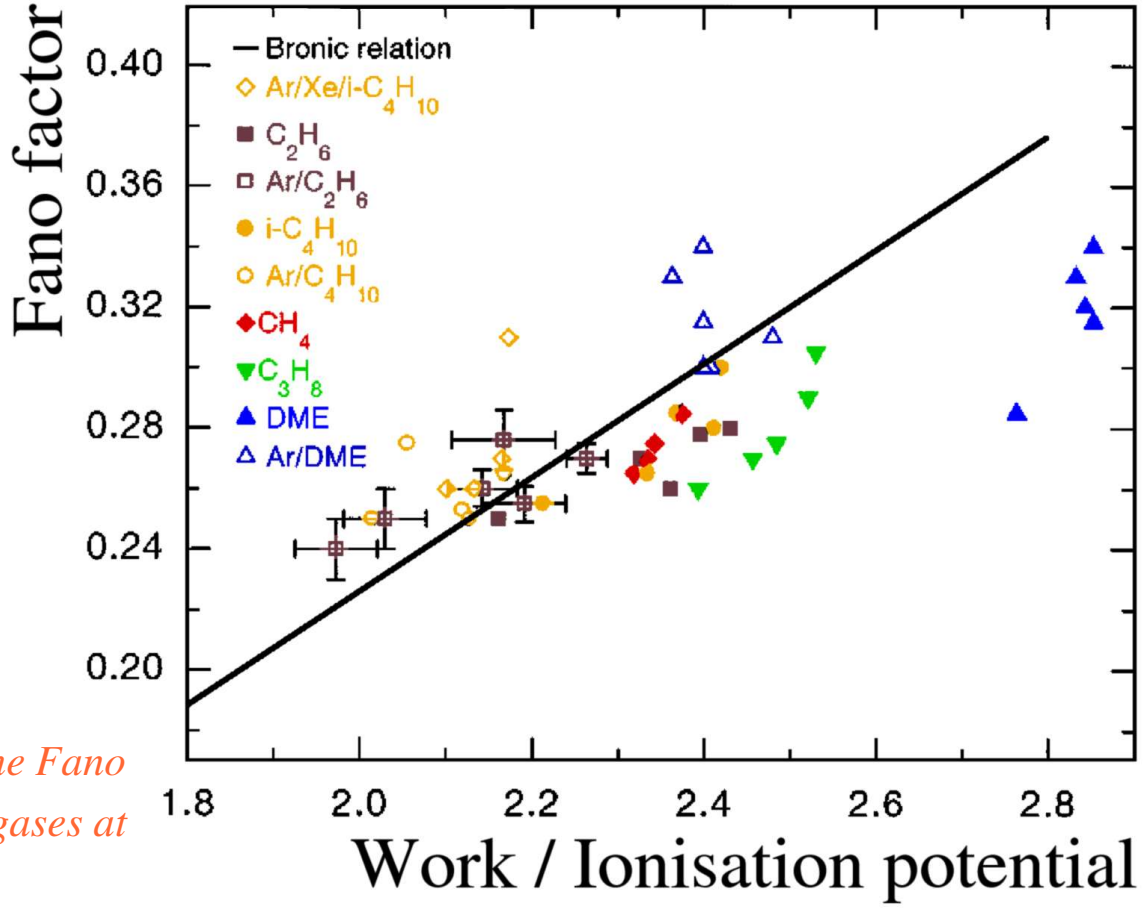

[Plot from: A. Pansky, A. Breskin and R. Chechik, *The Fano factor and the mean energy per ion-pair in counting gases at low X-ray energies,* J. Appl. Phys. **82** (1997) 871.]

Heed model

- For each path segment:
  - energy loss computed using Geant 3 algorithm,
  - draw a random energy needed for ionisation, from a "designer" distribution,
  - ionise if possible, subtract energy from δ-energy,
  - apply scattering,
  - repeat until all energy is consumed.

Energy used to ionise an atom

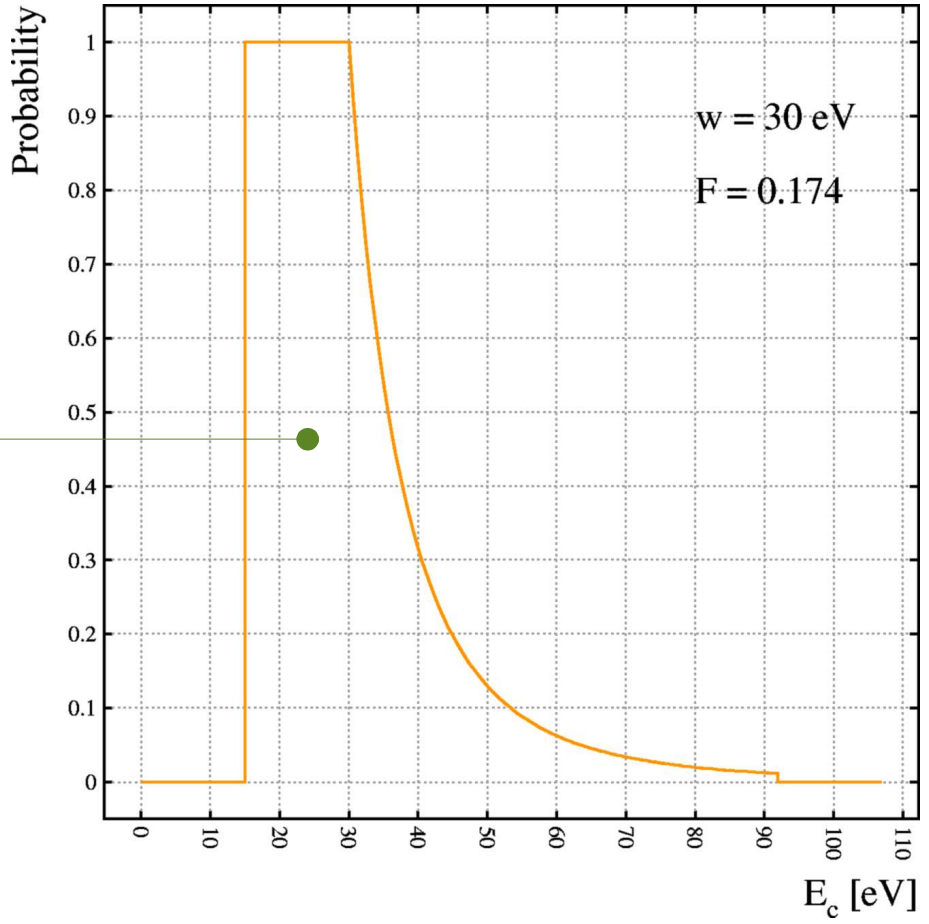

Work per electron in Heed

- The low-energy behaviour reflects the residual energy left in the δ-electron when it can not anymore ionise.
- Agrees with empirical models (ICRU report 31).

- For Heed reference settings: F=0.174, w=30 eV.

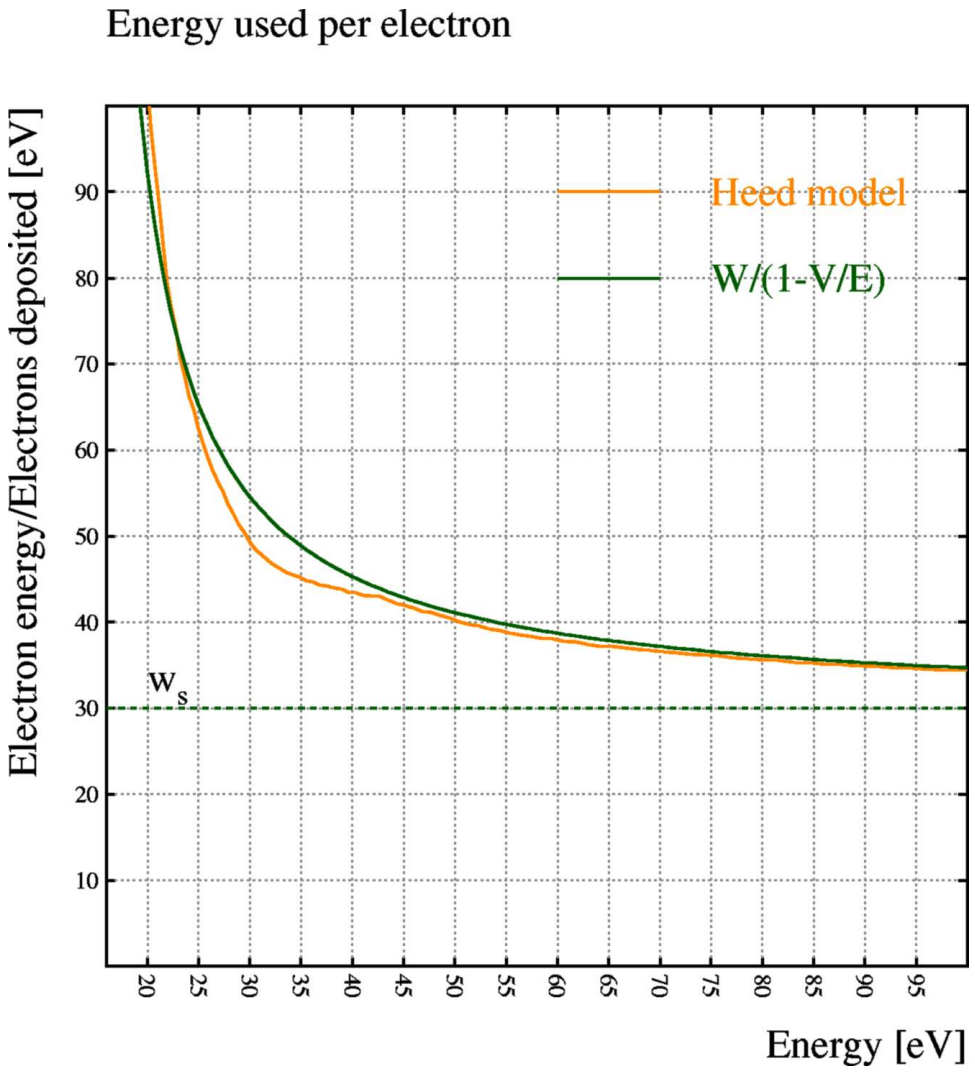

Fano factor: $F = RMS^2/mean$

Ugo Fano
(1912-2001)

- The total energy used for ionisation (and inelastic scattering) must not exceed the δ-energy. This limits the variance of the number of electrons deposited by a δ-electron.
  [U. Fano, Phys. Rev. **72** (1947) 26-29]
- This variance reduction is expressed in the Fano factor, F:
  - $F=1$ for a Poisson distribution,
  - larger in a molecular gas: inelastic collisions add degrees of freedom (exc. Penning transfers),
  - smaller in a noble gas,
  - falls with the energy of the δ-electron,
  - increases when the work needed to ionise is large with respect to the ionisation potential.

Fano factor in Heed

- No other ingredients than the ionisation energy distribution;
- Features the expected drop towards large energies;
- Plausible structure at low energies.

- For Heed reference settings: F=0.174, w=30 eV.

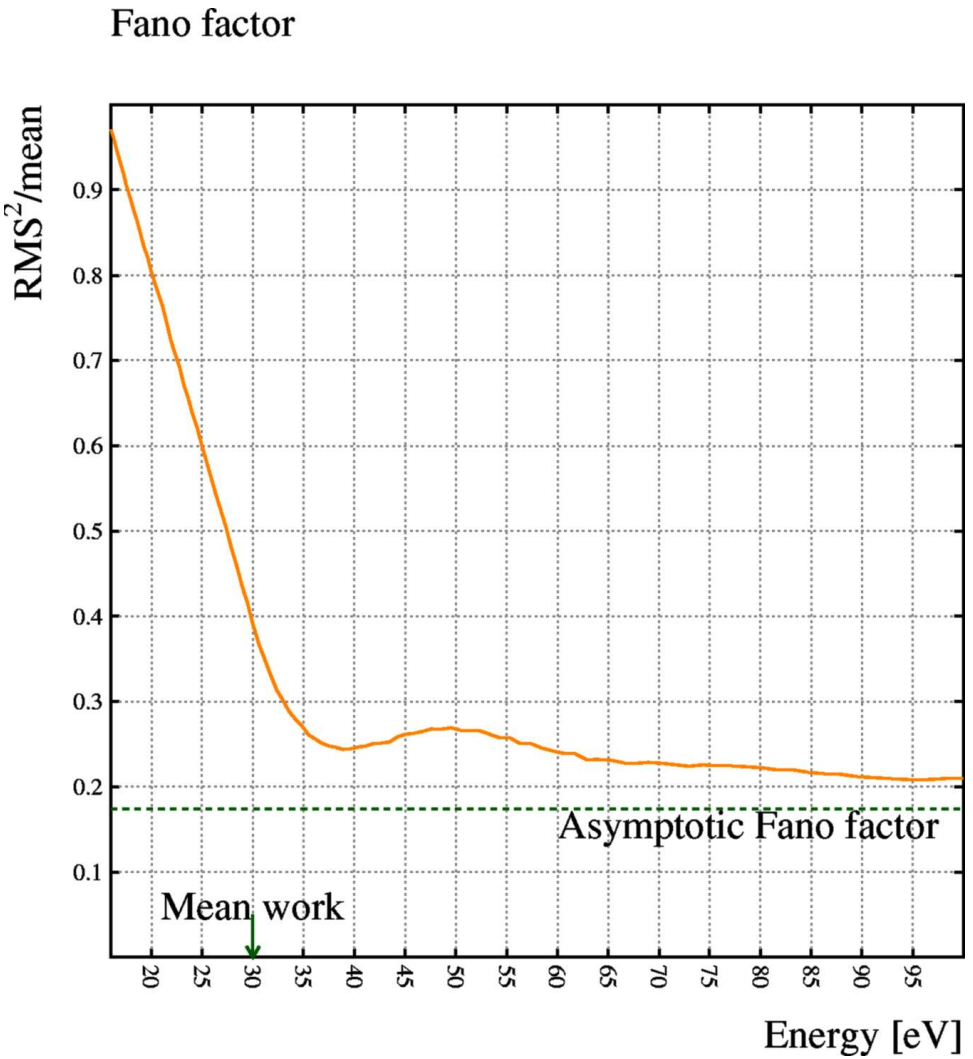

Field calculation techniques

- Analytic calculations:
  - almost all 2d structures made of wires, planes !
  - fast and precise, if applicable.
- Finite element method:
  - 2d and 3d structures, with or without dielectrics;
  - several major intrinsic shortcomings.
- Integral equations or Boundary element method:
  - equally comprehensive without the intrinsic flaws;
  - fraught with difficulties, not yet widely available.
- Finite differences:
  - still used for iterative, time-dependent calculations.

Analytic field calculations

- Analytic calculations rely on complex functions because of two remarkable properties:
  - Cauchy-Riemann equations:
    - The real part of *any* complex analytic function is a valid potential function.
  - Conformal mapping:
    - Almost *every* analytic geometric transformation of a valid potential, is a valid potential too.
- Applicability:
  - a surprisingly large class of detectors can be calculated with this technique: drift chambers, TPCs, MWPCs, hexagonal counters – but only in 2d.

Cauchy-Riemann equations

Augustin Louis Cauchy
(Aug 21st 1789 – May 23rd 1857)

- Express the existence of a derivative of a complex analytic function $f = u + \mathrm{i}\, v$

$$f'(z) = \frac{\partial f}{\partial x} = \frac{\partial u}{\partial x} + \mathrm{i}\frac{\partial v}{\partial x} \qquad \frac{\partial u}{\partial x} = \frac{\partial v}{\partial y}$$

$$= \frac{\partial f}{\partial \mathrm{i}\, y} = -\mathrm{i}\frac{\partial u}{\partial y} + \frac{\partial v}{\partial y} \qquad \frac{\partial v}{\partial x} = -\frac{\partial u}{\partial y}$$

Georg Friedrich Bernhard Riemann
(Sep 17st 1826 – Jul 20th 1866)

- Imply that u is harmonic:

$$\frac{\partial^2 u}{\partial x^2} = \frac{\partial^2 v}{\partial x \partial y} = \frac{\partial^2 v}{\partial y \partial x} = \frac{-\partial^2 u}{\partial y \partial y} \qquad \frac{\partial^2 u}{\partial x^2} + \frac{\partial^2 u}{\partial y^2} = 0$$

Jean le Rond d'Alembert
(Nov 16th 1717 –Oct 29th 1783)

- Reference: A.L. Cauchy, *Sur les intégrales définies* (1814). This *mémoire* was read in 1814, but only submitted to the printer in 1825.

Conformal mappings

- A geometric transformation through *any* analytic function maps any valid potential function to another, equally valid, potential function.

- Applications:
  - Cartesian to polar coordinates;
  - off-axis wire inside a tube;
  - external and internal areas of polygones;
  - ...

Conformal mappings - examples

- Schwarz-Christoffel transformation of a half-plane to the external part of a rectangle:

$$z \to \int_0^z \frac{\mathrm{d}\xi}{\sqrt{\xi(\xi-1)(\xi-a)}} = \frac{2}{\sqrt{a}} \mathrm{sn}^{-1}\left(\sqrt{z}, \frac{1}{\sqrt{a}}\right)$$

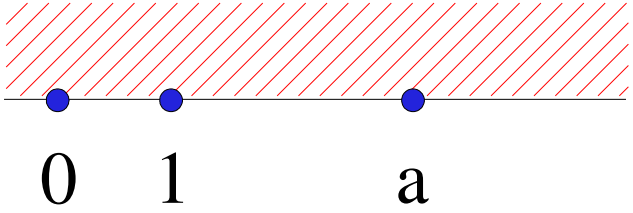

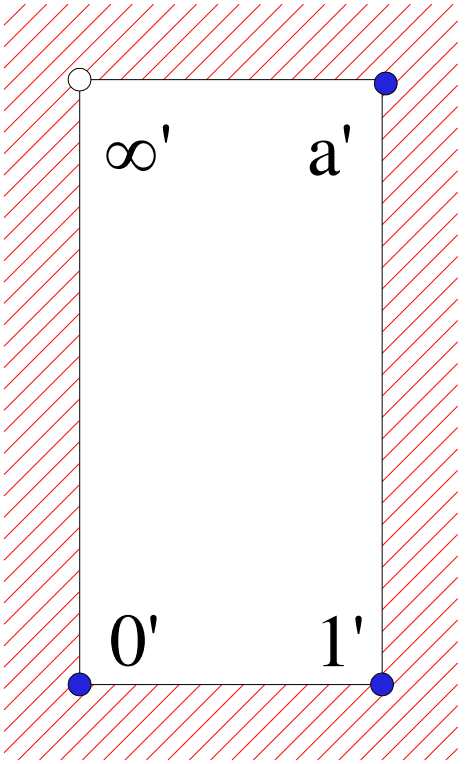

Why not 3d ?

Caspar Wessel (1745-1818)
Jean-Robert Argand (1768-1822)
Johann Carl Friedrich Gauss (1777-1855)
Sir William Rowan Hamilton (1805-1865)
Charles Sanders Peirce (1839-1914)
Georg Frobenius (1849-1917)

- The complex numbers $(\mathbb{R}^2,+,\times)$ form a field, like the real numbers $(\mathbb{R},+,\times)$, but $(\mathbb{R}^3,+,\times)$ does not. As a result, 2d arithmetic can be done with complex numbers, but there is no 3d equivalent for this.

- It can be proven that only $\mathbb{R}$ and $\mathbb{C}$ can form a commutative division algebra (field).

- $(\mathbb{R}^4,+,\times)$ can be made into a non-commutative division algebra known as quaternions, but this would not be help since $\nabla \cdot E$ links all dimensions.

Finite elements

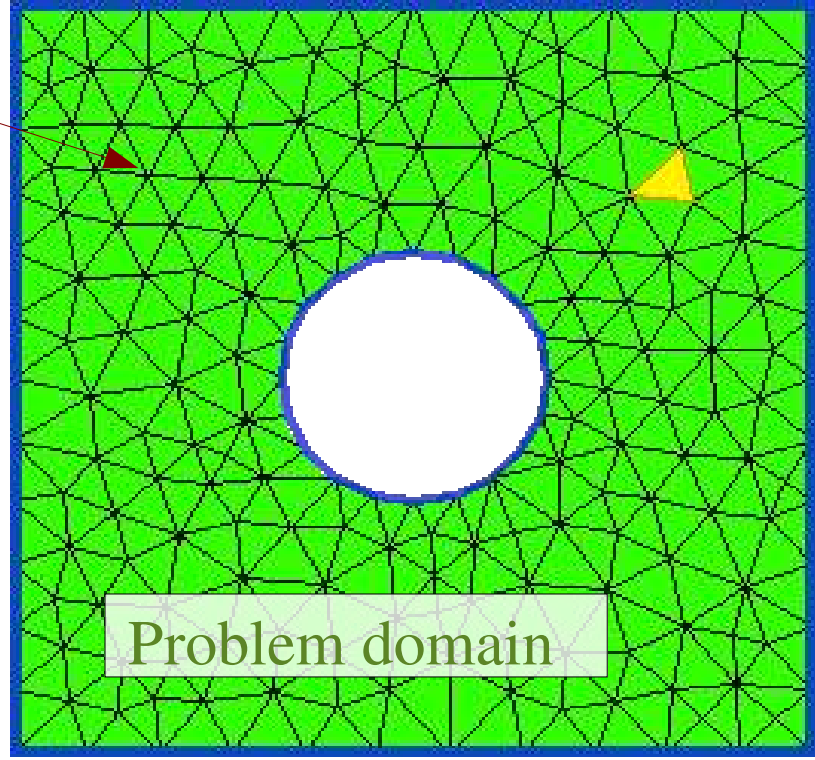

- A *mesh* subdivides the *problem domain* into *elements*.
- *Elements* are simple geometric shapes: triangles, squares, tetrahedra, hexahedra etc.
- Important points of *elements* are called *nodes*. It is usual that several *elements* have a *node* at one and the same location.

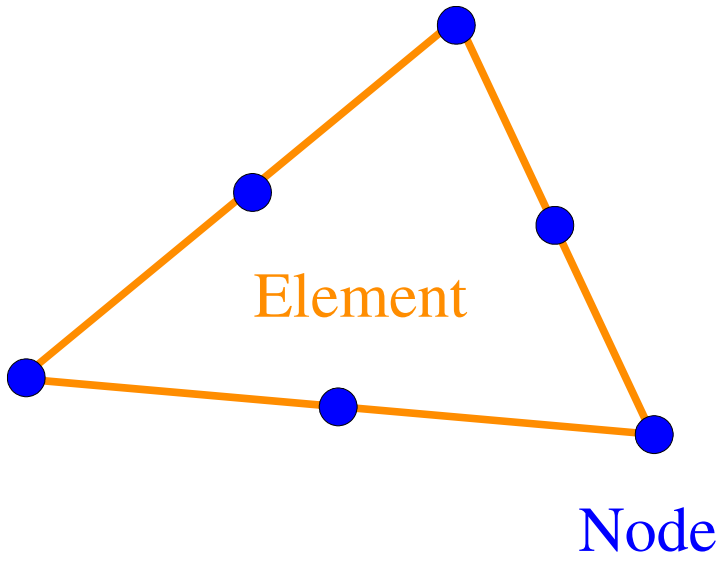

Shape functions - interpolation

- Each node has its own *shape function* $N_i(r)$:
  - continuous functions, usually polynomials,
  - defined only throughout the body of the element,
  - $N_i(r) = 1$ when $r = r_i$ i.e. on node i,
  - $N_i(r) = 0$ when $r = r_j$, $i \neq j$ i.e. on all other nodes.

- The solution of a finite element problem is given in the form of potential values at each of the nodes of each of the elements: v_i.

- At interior points of an element: $V(r) = \sum v_i N_i(r)$

Are polynomial N_i suitable for V ?

- Polynomial shape functions imply a polynomial potential, here a 3.2 cm tube + 30 μm wire at 3 kV:

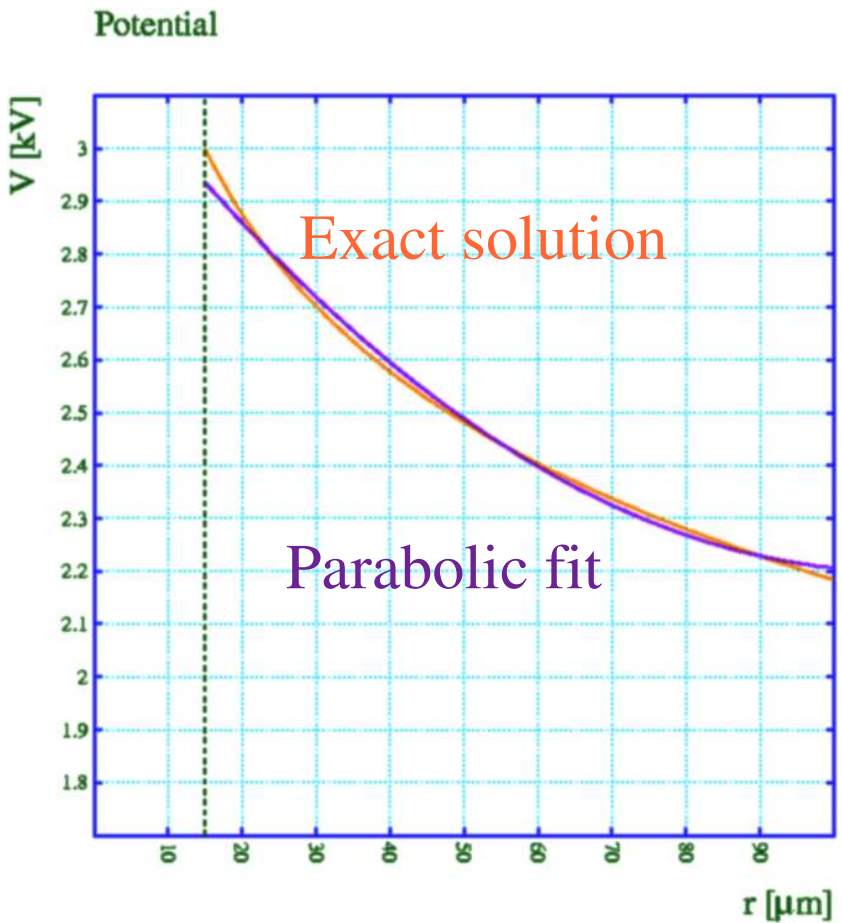

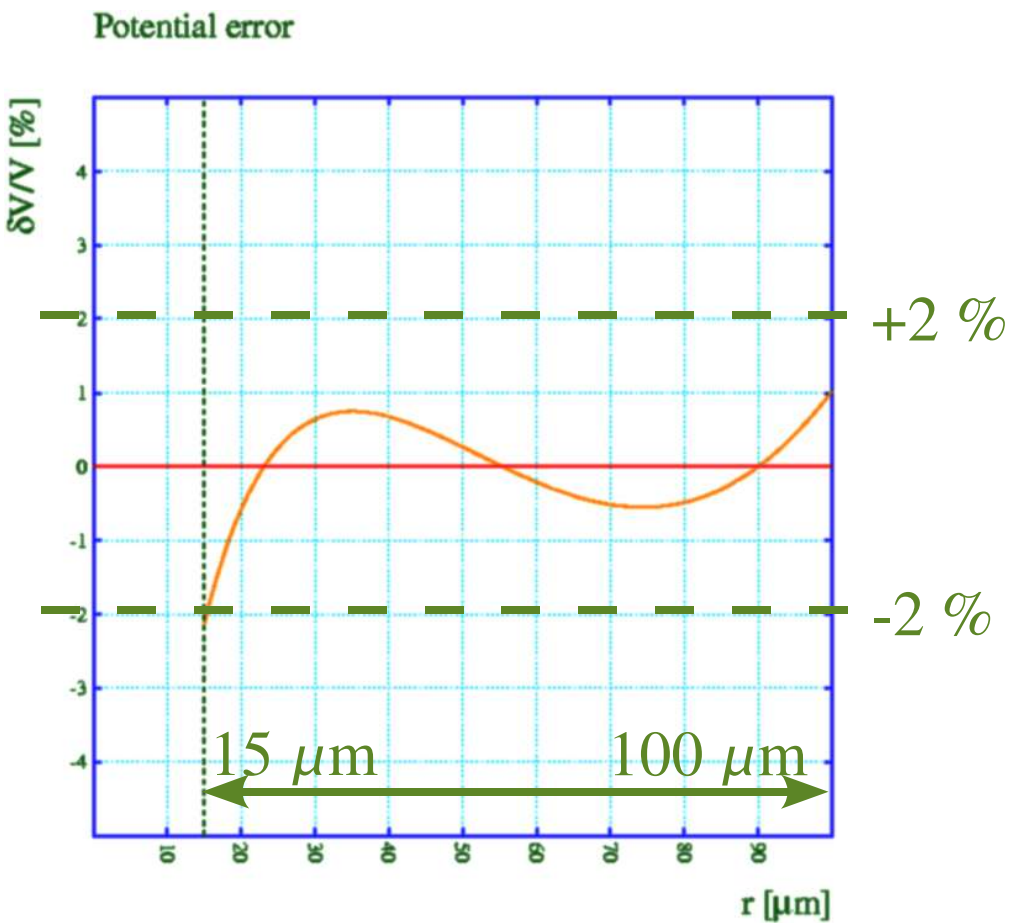

Are polynomial N_i suitable for E ?

- ... and a polynomial E field that is one order lower !

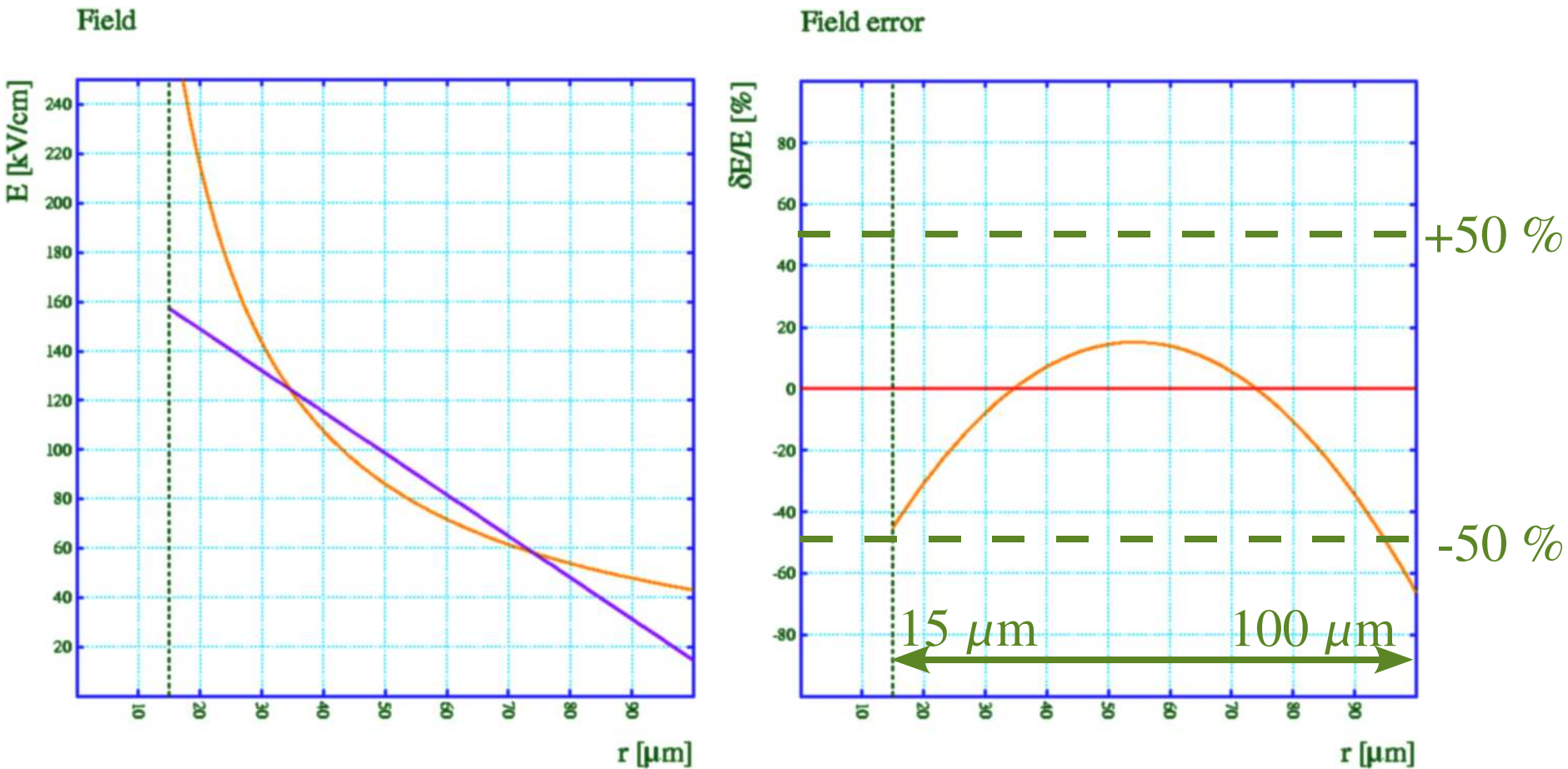

Continuity across boundaries

- Across element boundaries, the potential is guaranteed to be continuous.

- Example for a 2nd order triangle:
  - each edge shared by 2 elements, has 3 nodes;
  - the finite element method computes a unique potential for each node, i.e. the potential at the node is the same seen from both elements;
  - the potential is parabolic in each element, therefore also along each line in each element, and 3 points fully constrain a parabola.

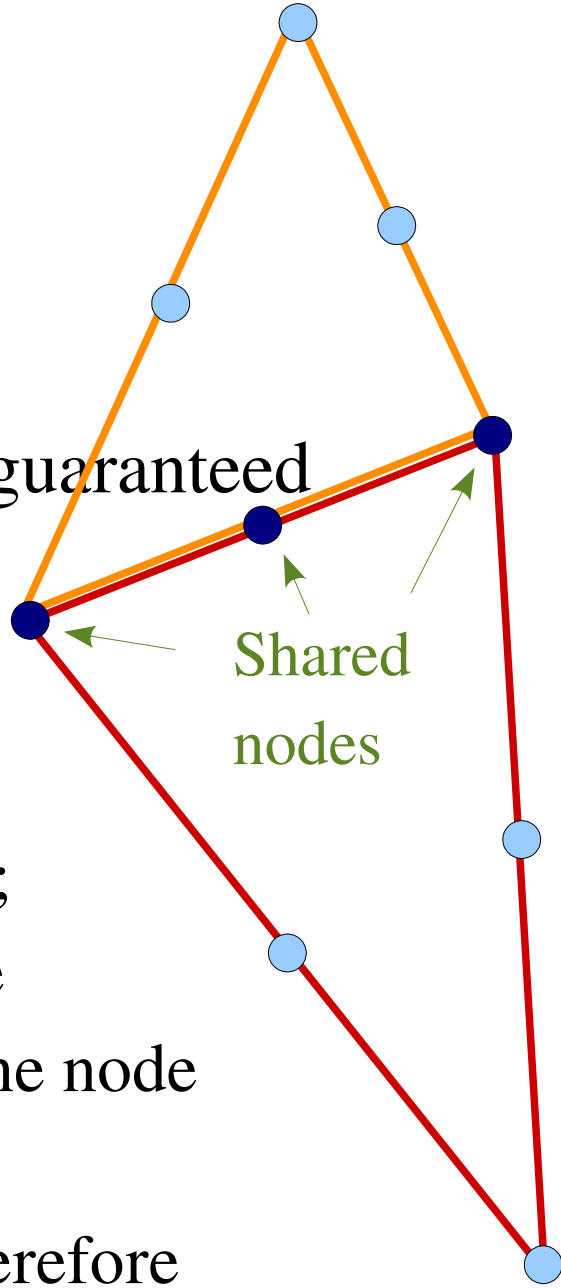

Continuity: the *E* field

- But ... the components of the *E* field look like the roofs of Nice: locally linear, and discontinuous.

Photo from: http://www.06nice.com/somvol/fotaer/gfoaer.htm

The price to pay for finite elements

- Finite element programs focus on the wrong thing:
  - they solve V well, but we do not really need it:
    - Quadratic shape functions can do a fair job at approximating $V \approx \log(r)$ potentials.
    - Potentials are continuous.
  - E is what we use, but:
    - Gradients of quadratic shape functions are linear and unsuitable to approximate our $E \approx 1/r$ fields with, left alone $E \approx 1/r^2$ fields.
    - Electric fields are discontinuous.
    - A local accuracy of ~50 % in high-field areas is perfectly normal.

Drift Field

Poisson equation

$$\nabla \cdot (\epsilon E) = \frac{\rho}{\epsilon_0}$$

electrons, acceptors

$$\rho = e(p - n + N_D - N_A) + \rho_t$$

holes, donors, traps, fixed charges

iterative calculation of drift field

Continuity equation (drift-diffusion model)

$$j_n = n \mu_n E - D_n \nabla n \qquad j_p = -p \mu_p E - D_p \nabla p$$

$$\frac{\partial n}{\partial t} = -\nabla \cdot j_n + G_n - R_n \qquad \frac{\partial p}{\partial t} = -\nabla \cdot j_p + G_p - R_p$$

TCAD

Synopsys TCAD (http://www.synopsys.com/Tools/TCAD/Pages/default.aspx): part of Sentaurus process and device simulation package

Create device structure (materials and contacts) and define doping concentrations → meshing → apply boundary conditions, select physical models to be used (e.g. mobility, impurities, charge deposition→ iterative numerical solution of Poisson equation + continuity equations for given boundary conditions
provides an extensive set of physical models → very valuable as reference

Example: silicon strip detector

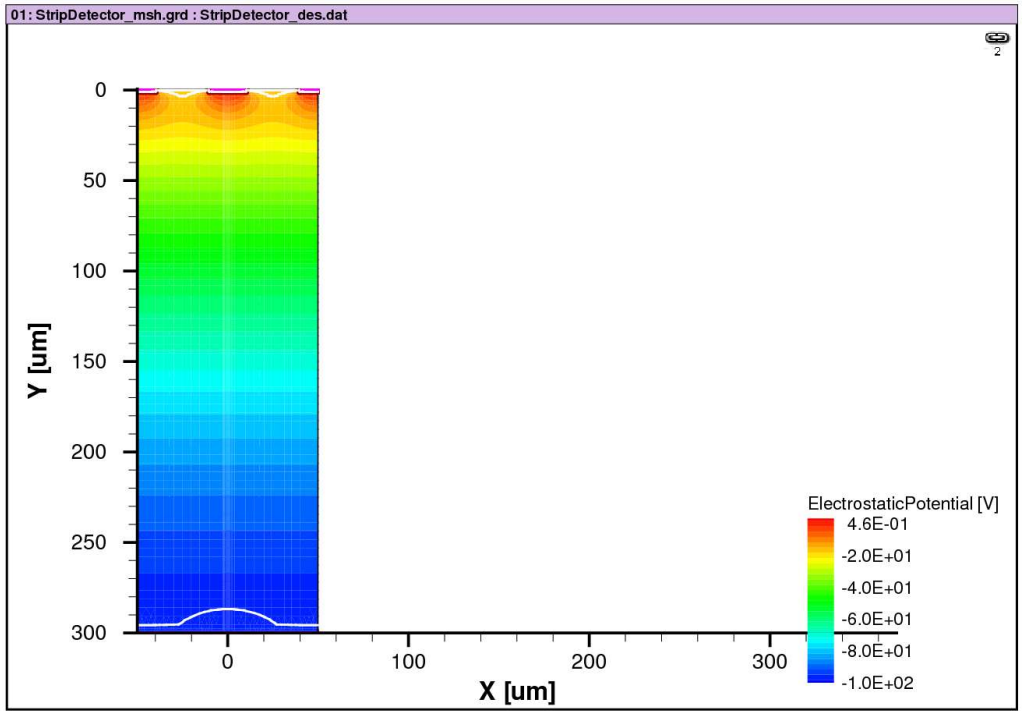

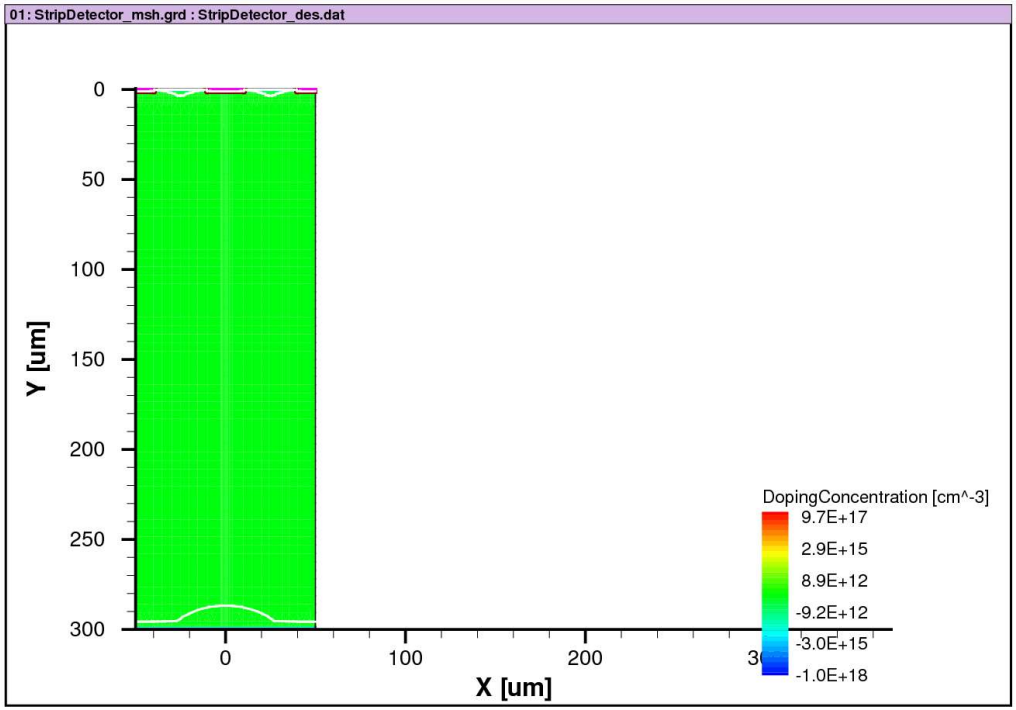

from http://ppewww.physics.gla.ac.uk/det_dev/activities/threedee/Documents/BarcelonaSeminar.html

Boundary element methods

- Contrary to the finite element method, the elements are on the boundaries, not in the problem domain itself.
- Charges are computed for the boundary elements.

- The fields in the problem domain are calculated as the sum of Maxwell-compliant field functions, not polynomials. There are therefore no discontinuities.

- In contrast, they tend to pose bigger numerical challenges due to inherent singularities.

Solution of 3D Poisson's Equation

using BEM

- Numerical implementation of boundary integral equations (BIE) based on Green's function by discretization of boundary.
- Boundary elements endowed with distribution of sources, doublets, dipoles, vortices.

Electrostatics BIE

$$\phi(\vec{r}) = \int_S G(\vec{r}, \vec{r}\,')\rho(\vec{r}\,')\,dS'$$

Potential at r

Charge density at r'

Green's function

$$G(\vec{r}, \vec{r}\,') = \frac{1}{4\pi\epsilon|\vec{r} - \vec{r}\,'|}$$

ε - permittivity of medium

discretization

$$[A]\{\rho\} = \{\phi\}$$

Influence Coefficient Matrix

$$\{\rho\} = [A]^{-1}\{\phi\}$$

Accuracy depends critically on the estimation of [A], in turn, the integration of G, which involves singularities when r → r'.

Most BEM solvers fail here.

Eletrostatics of Micromegas

FEM Results

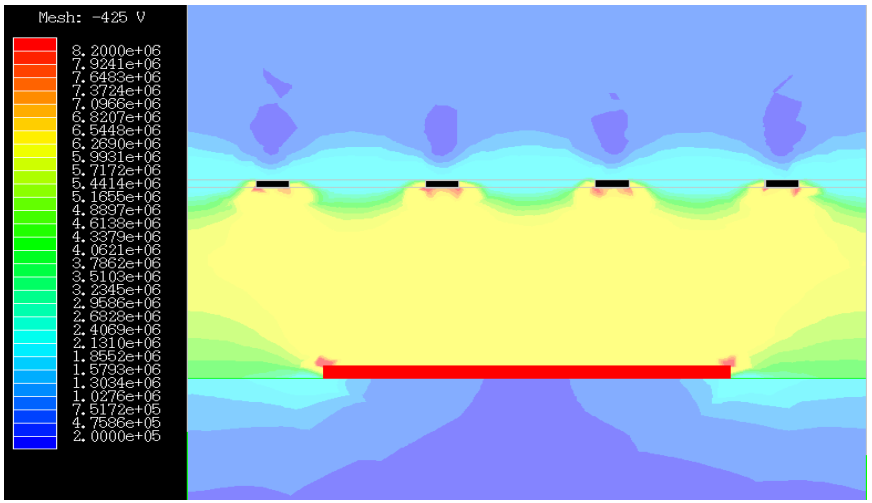

Electric field along hole-centered path line

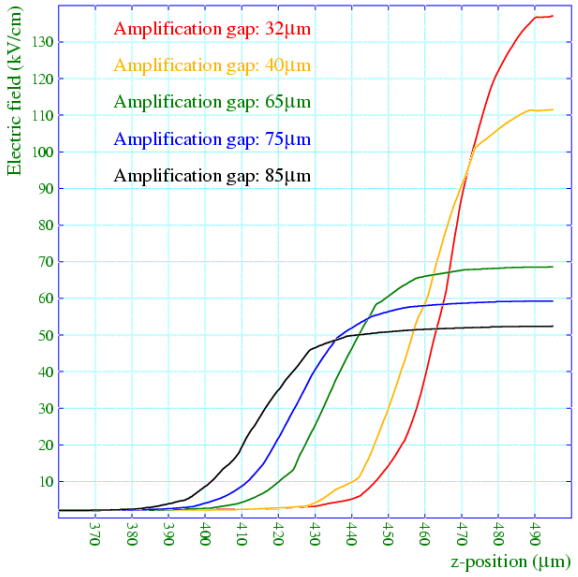

neBEM Results

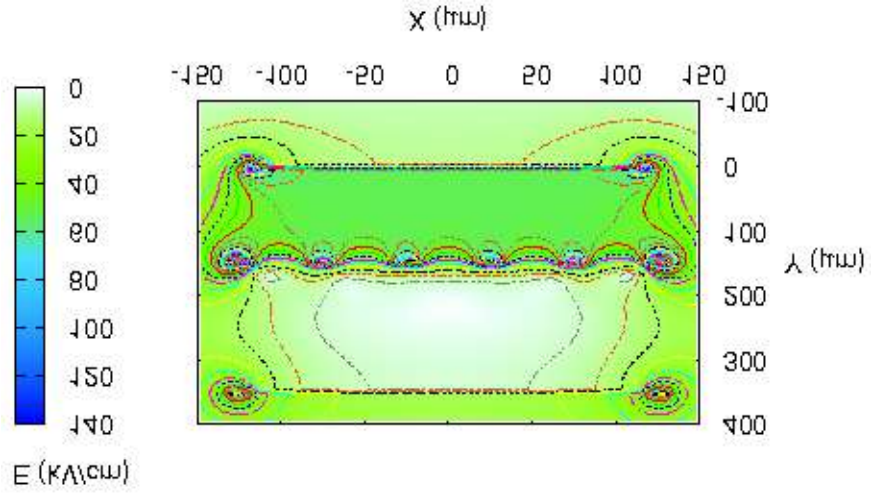

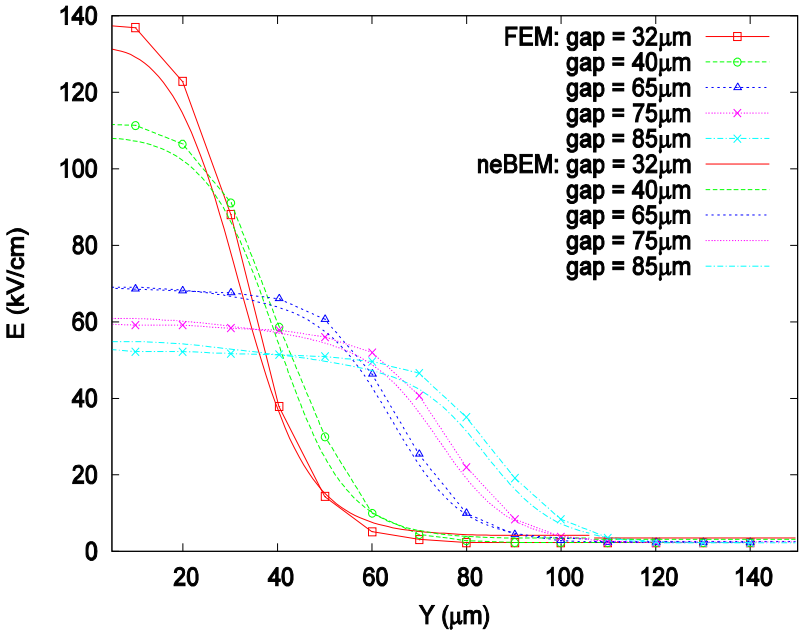

Ar: mean free path

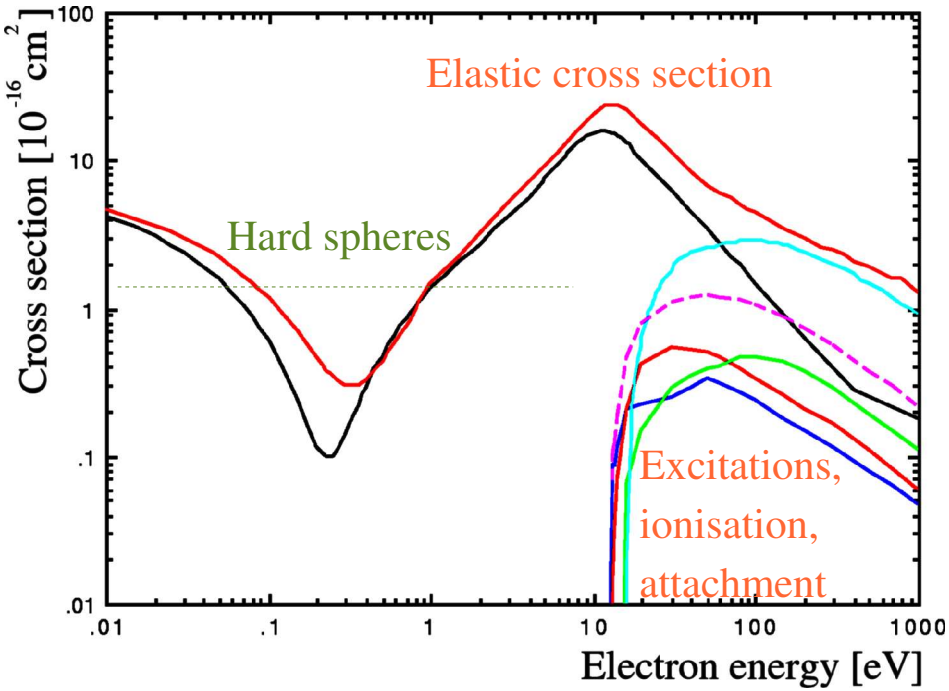

- Using:
  - atomic radius: $r \approx 70$ pm
  - atomic cross section: $\sigma \approx 1.5\ 10^{-16}$ cm^2
  - atoms per volume: $\mathscr{L} \approx 2.7\ 10^{19}$ atoms/cm^3
- Over a distance L, the electron hits $\mathscr{L}\sigma L$ atoms.
- Hence, the mean free path is $\lambda_e = 1/(\mathscr{L}\sigma) \approx 2\ \mu$m.

Scale ≫ mean free path (> 1 mm)

- For practical purposes, electrons from a given starting point reach the same electrode – but with a spread in time and gain.

- Electrons transport is treated by:
  - integrating the equation of motion, using the Runge-Kutta-Fehlberg method, to obtain the path;
  - integrating the diffusion and Townsend coefficients to obtain spread and gain.

- This approach is adequate for TPCs, drift tubes etc.

Runge-Kutta-Fehlberg integration

- Example: a TPC read-out cell

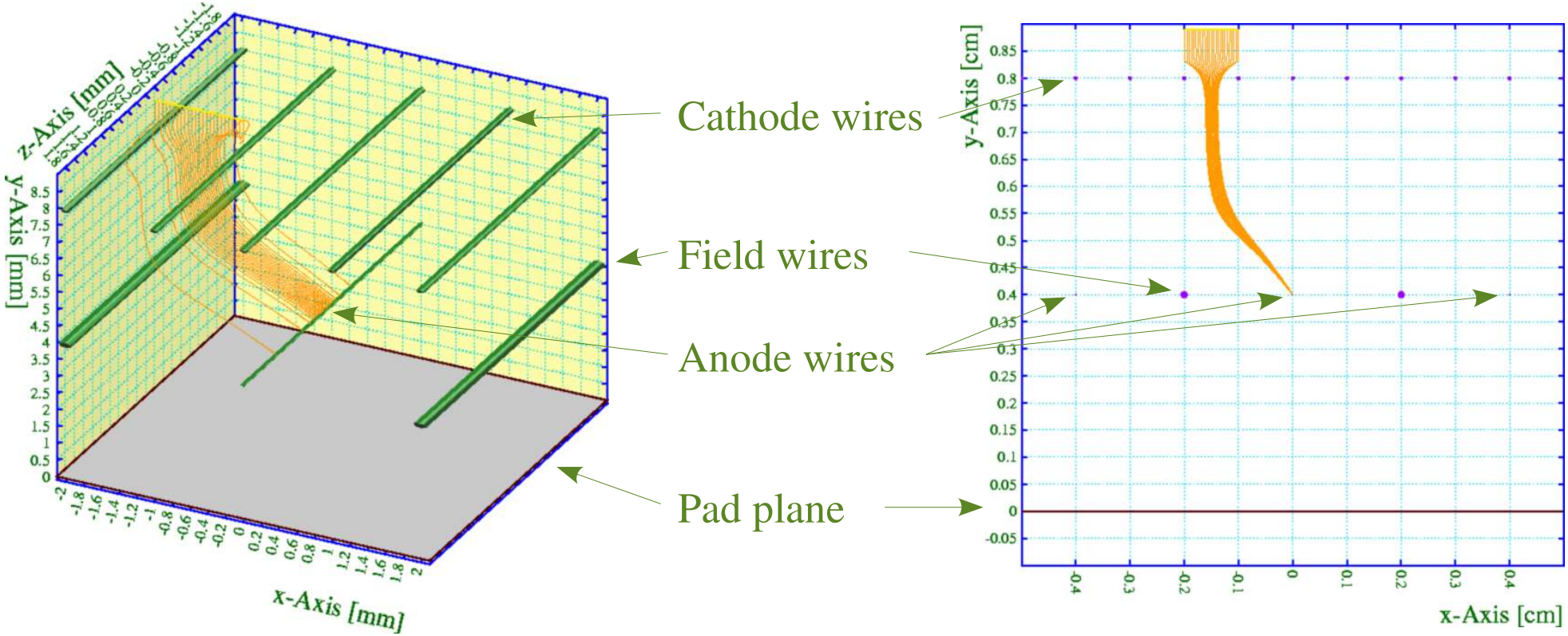

Scale > mean free path (100 μm - 1 mm)

- Electrons from a single starting point may end up on any of several electrodes.
- Calculations use Monte Carlo techniques, based on the mean drift velocity and the diffusion tensor computed by microscopic integration of the equation of motion in a constant field. Gain depends on the path.
- This approach is adequate as long as the drift field is locally constant – a reasonably valid assumption in a Micromegas but less so in a GEM.

Analytic vs Monte Carlo

- Analytic integration
  - Runge-Kutta-Fehlberg technique;
  - automatically adjusted step size;
  - optional integration of diffusion, multiplication and losses.

- Monte Carlo integration
  - non-Gaussian in accelerating, divergent and convergent fields;
  - step size to be set by user.

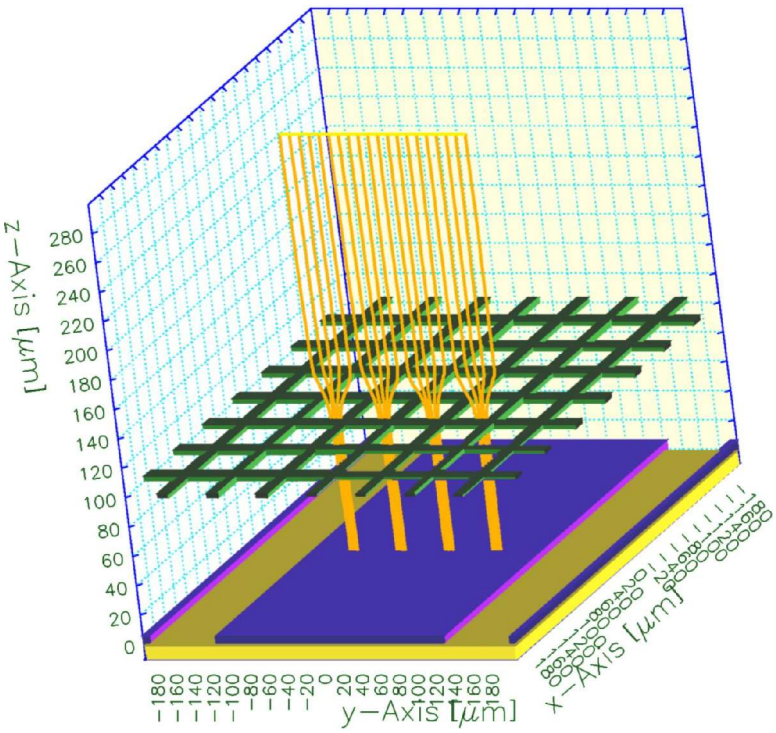

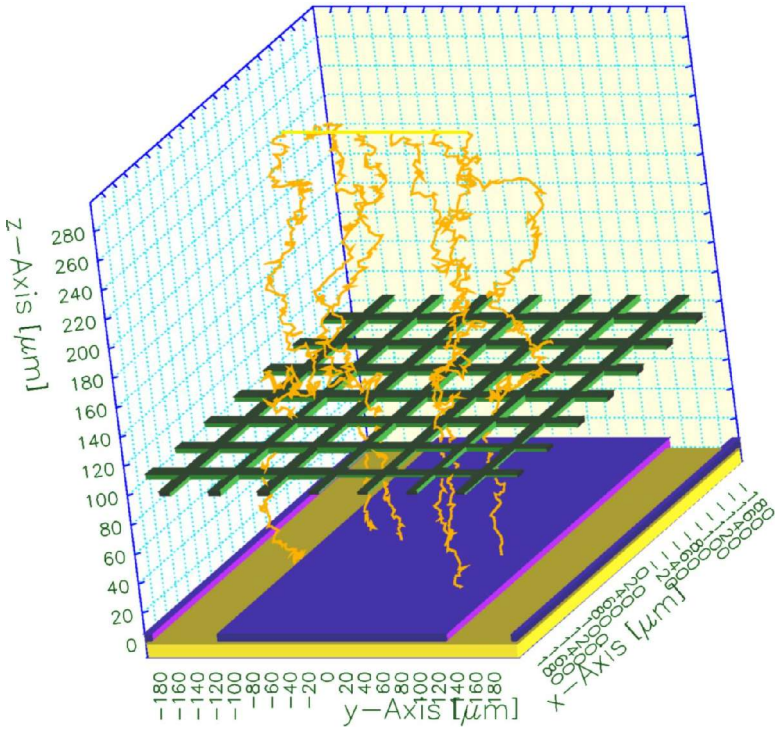

[Figures made by Gilles Barouch, CEA]

Scale ~ mean free path (1-100 μm)

- At this scale, where the mean free path approaches the characteristic dimensions of detector elements, free flight between collisions, is no longer be parabolic.

- The only viable approach here seems to be a complete microscopic simulation of the transport processes, taking local field variations into account.

- The method shown here is based on the Magboltz program.

Molecular tracking: example

- Example:
  - CSC-like structure,
  - Ar 80 % CO_2 20 %,
  - 10 GeV μ.
- The electron is shown every 100 collisions, but has been tracked rigourously.

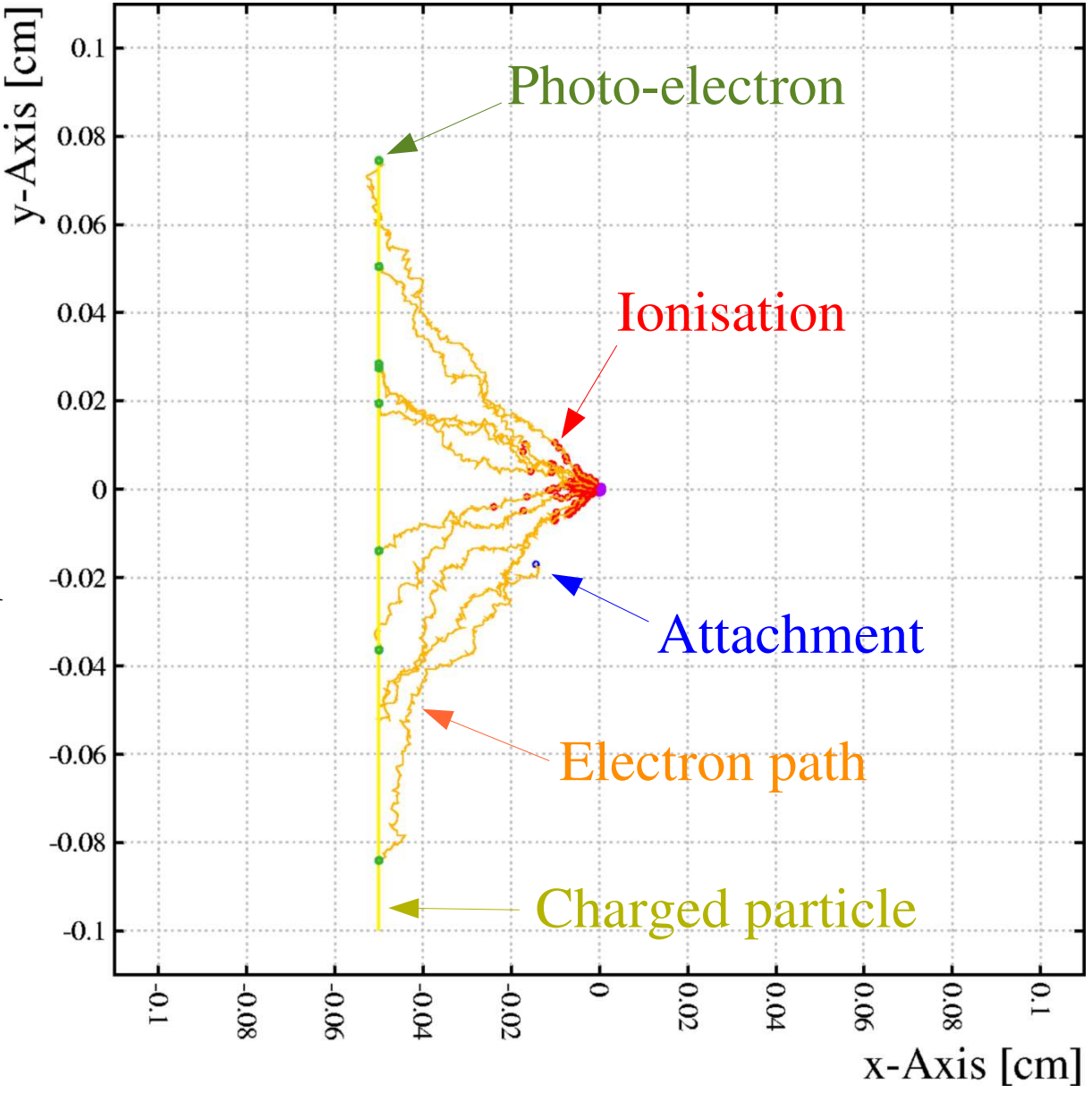

What is in the Magboltz database ?

- A large number of cross sections for 60 molecules...
  - All noble gases, *e.g.* argon:
    - elastic scattering,
    - 3 excited states and
    - ionisation.
  - Numerous organic gases, additives, *e.g.* CO_2:
    - elastic scattering,
    - 44 inelastic cross sections (vibrations, rotations, polyads)
    - 35 super-elastic cross sections,
    - 6 excited states,
    - attachment and
    - ionisation.

Argon

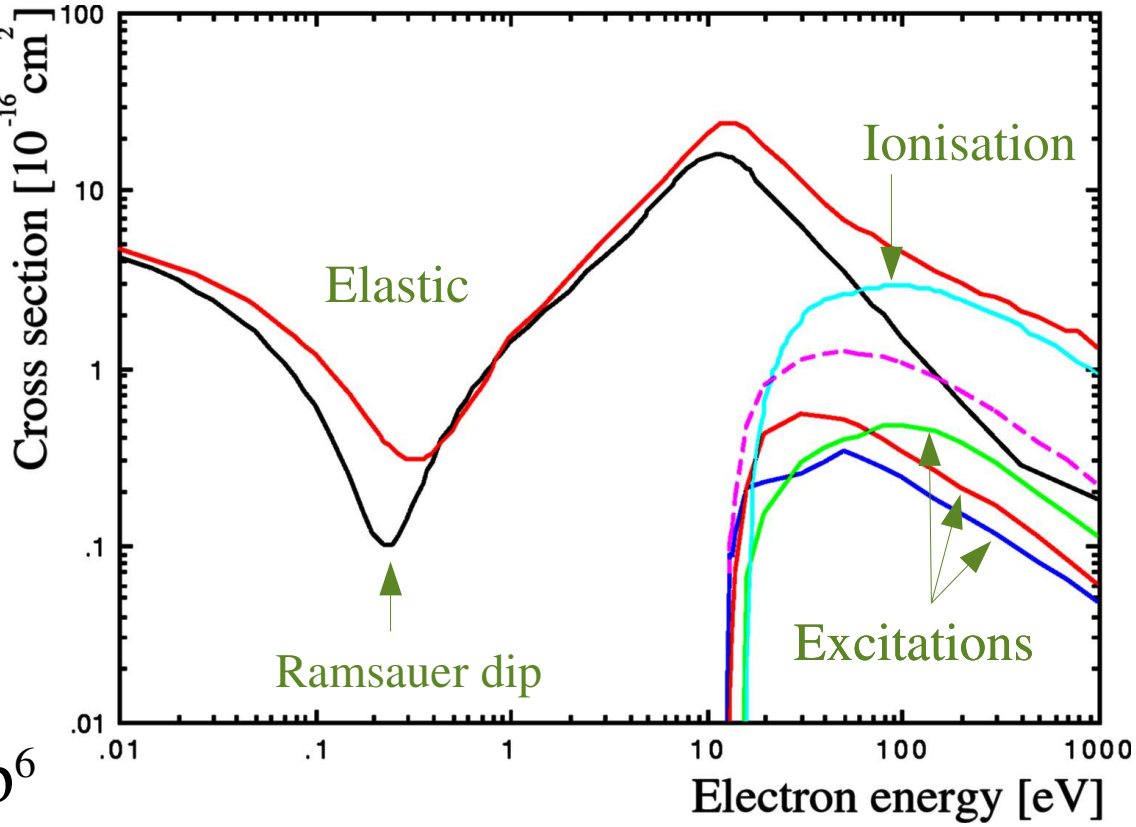

- Elastic scattering:
  - dominant till ~50 eV;
  - features Ramsauer dip
- Ground state: [Ne] $3s^2\,3p^6$

  the lowest excited states have an e^- in the
  - 3rd shell: [Ne] $3s^2\,3p^5\,3d^1$, or
  - 4th shell: [Ne] $3s^2\,3p^5\,4s^1$, [Ne] $3s^2\,3p^5\,4p^1$, ...
- Attachment is not significant.
- Ionisation
  - occurs from 15.7 eV;
  - 2 levels: $3p^5$ spin and orbital angular momentum ↑↑ or ↑↓.

Argon levels

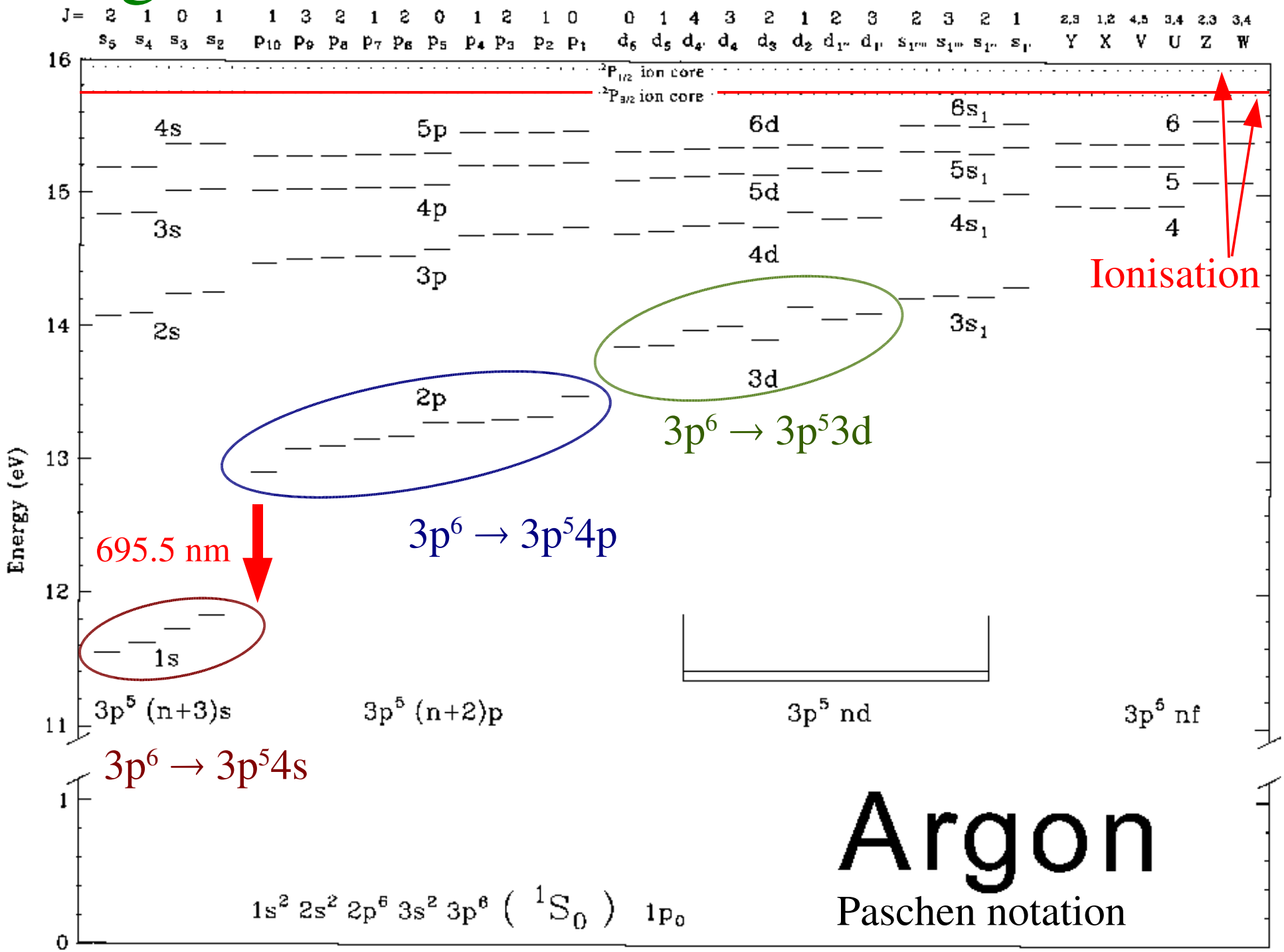

CO_2 – vibration modes

- CO_2 is linear:
  - O – C – O
- Vibration modes are numbered V(*ijk*)
  - *i*: symmetric,
  - *j*: bending,
  - *k*: anti-symmetric.

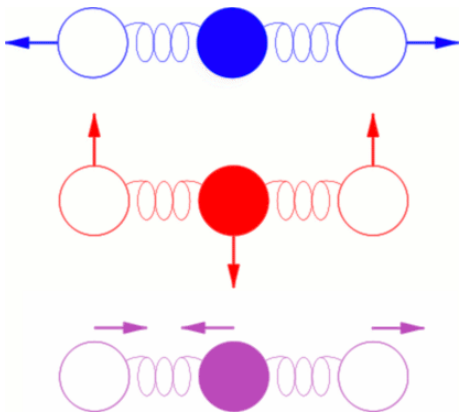

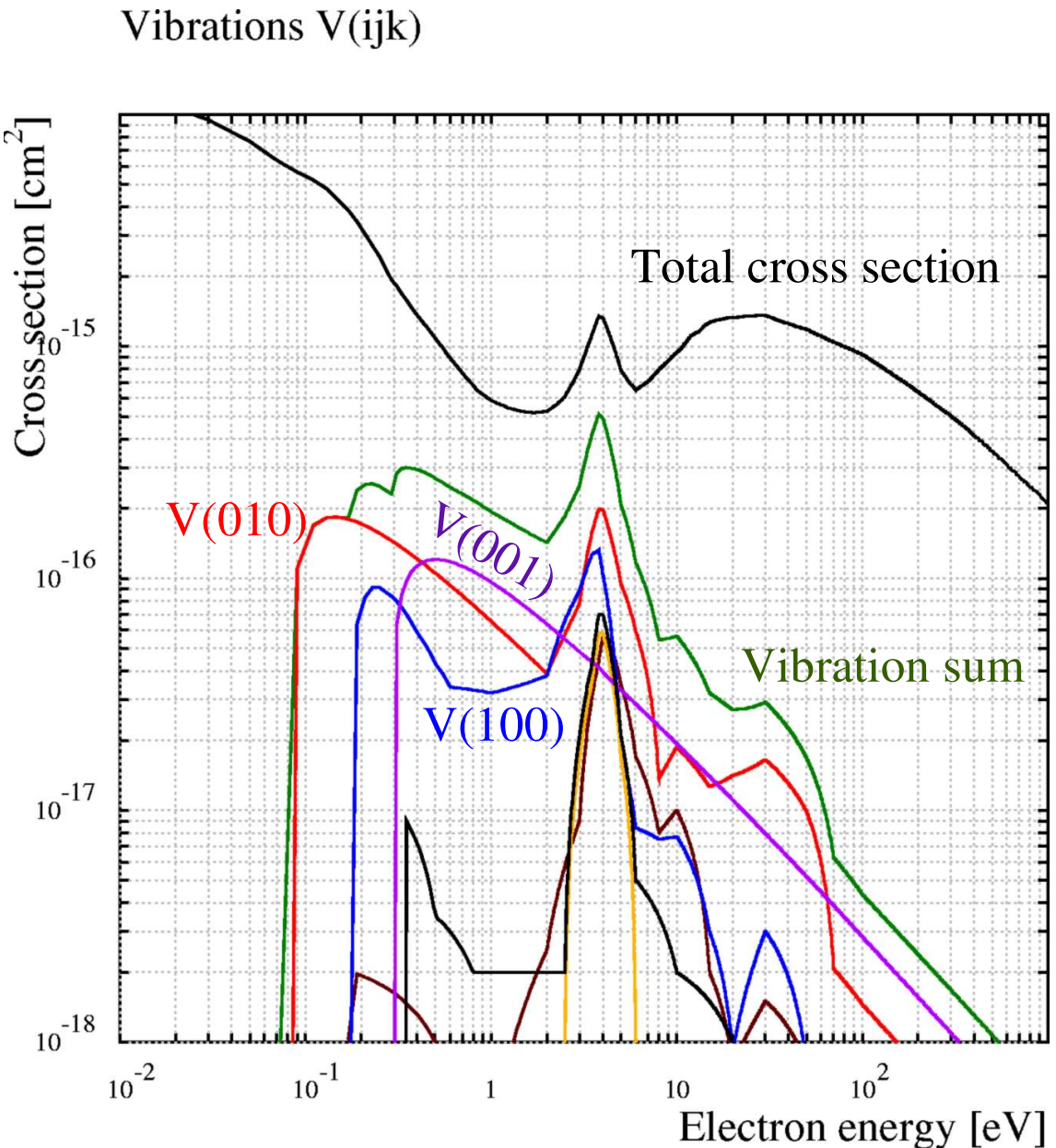

Signal properties

- Properties of the current induced in an electrode:
  - proportional to the charge Q;
  - proportional to the velocity of the charge $\vec{v}_{\mathrm{d}}$;
  - dependent on the electrode and the geometry.
- This leads to the following ansatz:

$$I = -Q\,\vec{v}_{\mathrm{d}} \cdot \vec{E}_{\mathrm{w}}$$

- The geometry is contained in $\vec{E}_{\mathrm{w}}$, by construction a vectorial quantity, the *weighting field*. Each electrode has its own weighting field.
- The sign is mere convention.

NA49 measured signal

- Apparently, many ions go to the field wires.
- Dominant ion species is Ne^+, not the faster CO_2^+.

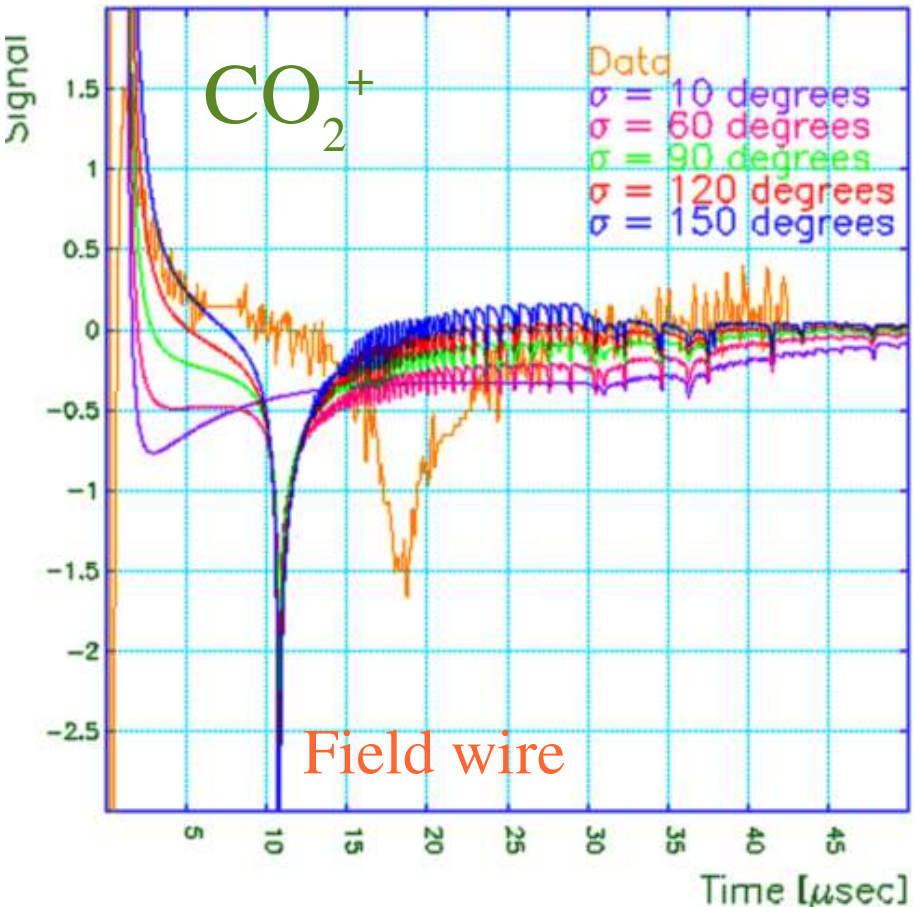

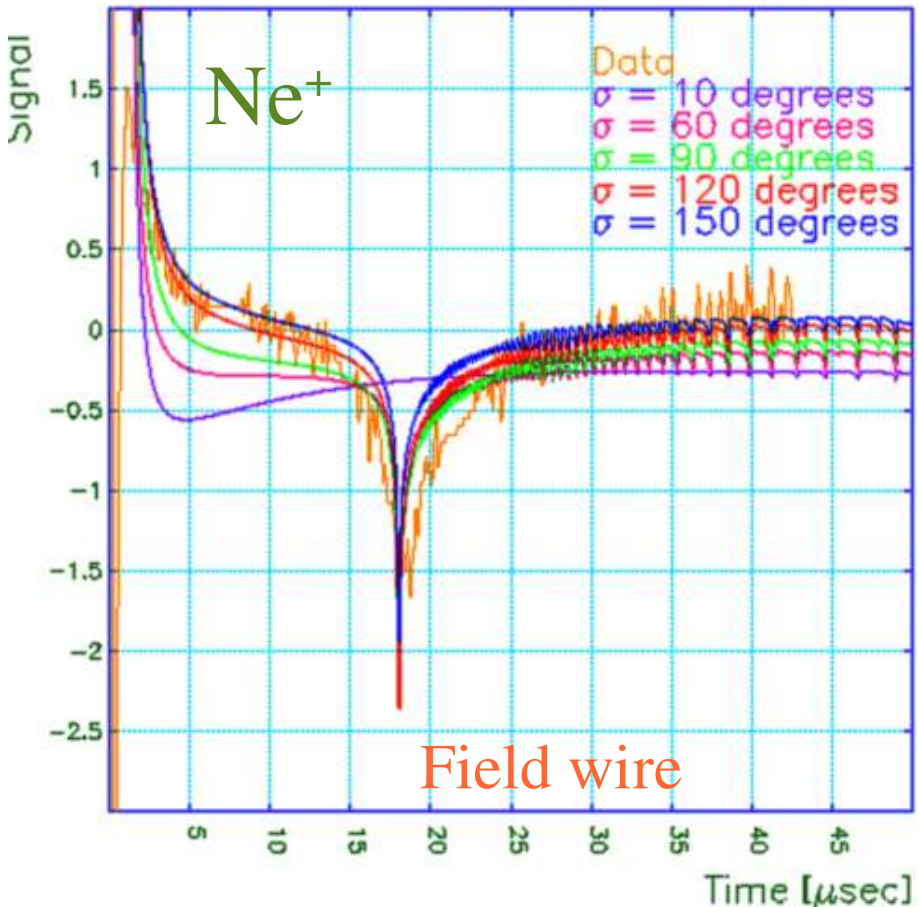

Summary

- Inspite of the long history of gas-based detectors, understanding of their behaviour still improves.
- Calculations for gas detectors are therefore steadily becoming more detailed, and it becomes more and more important for the users to understand the model.
- In some domains, *e.g.* signal shapes, one can easily verify the calculations by hand. In others, *e.g.* the gas properties, this is unfortunately far from trivial.